Copyright Warning & Restrictions

The copyright law of the United States (Title 17, United States Code) governs the making of photocopies or other reproductions of copyrighted material.

Under certain conditions specified in the law, libraries and archives are authorized to furnish a photocopy or other reproduction. One of these specified conditions is that the photocopy or reproduction is not to be "used for any purpose other than private study, scholarship, or research." If a, user makes a request for, or later uses, a photocopy or reproduction for purposes in excess of "fair use" that user may be liable for copyright infringement,

This institution reserves the right to refuse to accept a copying order if, in its judgment, fulfillment of the order would involve violation of copyright law.

Please Note: The author retains the copyright while the New Jersey Institute of Technology reserves the right to distribute this thesis or dissertation

Printing note: If you do not wish to print this page, then select "Pages from: first page # to: last page #" on the print dialog screen

ABSTRACT

ASSESSING STRUCTURAL AND FUNCTIONAL BRAIN ALTERATIONS AND WORK-RELATED FATIGUE IN NON-HYPOSMIC AND HYPOSMIC COVID-19 SURVIVORS

by
Rakibul Hafiz

In the year 2019, life began to change at the advent of a global pandemic caused by the novel coronavirus. Mask mandates and mass vaccinations have mitigated the effects significantly, yet cases keep rising with new variants, especially, in densely populated countries, like India. Recent neuroimaging evidence shows the virus can attack the central nervous system (CNS). However, exactly which brain regions undergo structural and functional changes remain largely unknown. Many patients experience 'loss of/reduced sense of smell' (i.e., hyposmic) and an alarming number of survivors develop persistent symptoms ('long-COVID') for several months after initial infection. Fatigue is the most reported symptom among several others that show signs of cognitive deficits. Therefore, how these brain alterations differ among healthy controls and patient subtypes (non-hyposmic and hyposmic) and how they relate to fatigue need to be investigated.

To address these gaps, 35 healthy controls and 47 COVID-19 survivors, two weeks after hospital discharge, are recruited from a single site located at Delhi, India. T1-weighted structural magnetic resonance imaging (MRI) and resting state functional MRI (RS-fMRI) are used to test our hypothesis that brain structure and function change across healthy, non-hyposmic and hyposmic groups. Furthermore, correlations of structural and functional brain imaging metrics with self-reported fatigue at work are reported. Fatigue levels are higher in the COVID group (hyposmic and non-hyposmic) compared to the healthy group

($p < 0.05$). For the structural morphometry analysis, ANOVA reveals differences in global gray matter volume (GMV) across groups ($F = 3.48, p < 0.05$), which is observed to be higher in the hyposmic group from post-hoc tests. After controlling for age, sex and total intracranial volume (TIV), voxel-based morphometry (VBM) reveals four clusters ($p_{FWE} < 0.05$) from the ANOVA analysis comprising regions from the *limbic system*, *occipitotemporal* and *cerebellar* lobes. Post-hoc analysis on these clusters reveal that hyposmic patients have higher GMV compared to non-hyposmic and healthy control groups. Furthermore, the COVID group demonstrate stronger correlation of fatigue with GMV ($\rho = 0.41, p < 0.05$) within *precuneus*, *posterior cingulate cortex* and *superior parietal lobule*. From functional data analysis, amplitude of low frequency fluctuations (ALFF) is higher in the hyposmic and non-hyposmic groups compared to the healthy controls, within the *limbic system* and *basal ganglia.* Functional connectivity (FC) derived from independent component analysis (ICA) is reduced in the hyposmic group, compared to both non-hyposmic and healthy groups with *medial* and *orbito-frontal* regions for the *basal ganglia network.* On the other hand, the hyposmic group show enhanced FC compared to healthy and non-hyposmic groups within the *precuneus* and *somato-sensory* networks*,* respectively. Moreover, the FC of the *superior parietal lobule*, is negatively correlated with work-related fatigue ($\rho = -0.47, p < 0.05$) for the *precuneus* network. The results indicate that COVID survivors demonstrate brain alterations at an early stage of recovery and more strongly correlate with work-related fatigue, which can be an early marker for 'long-COVID'. Altered brain regions observed from this study also match with clinical MRI reports and current fMRI literature, suggesting these findings could have relevance to both clinical diagnosis and research related investigations.

ASSESSING STRUCTURAL AND FUNCTIONAL BRAIN ALTERATIONS AND WORK-RELATED FATIGUE IN NON-HYPOSMIC AND HYPOSMIC COVID-19 SURVIVORS

by
Rakibul Hafiz

A Dissertation
Submitted to the Faculty of
New Jersey Institute of Technology
And Rutgers University Biomedical and Health Sciences – Newark
in Partial Fulfillment of the Requirements for the Degree of
Doctor of Philosophy in Biomedical Engineering

Department of Biomedical Engineering

May 2022

APPROVAL PAGE

ASSESSING STRUCTURAL AND FUNCTIONAL BRAIN ALTERATIONS AND WORK-RELATED FATIGUE IN NON-HYPOSMIC AND HYPOSMIC COVID-19 SURVIVORS

Rakibul Hafiz

Dr. Bharat B. Biswal, Dissertation Co-Advisor Distinguished Professor of Biomedical Engineering, NJIT	Date
Dr. Xiaobo Li, Dissertation Co-Advisor Associate Professor of Biomedical Engineering, NJIT	Date
Dr. Tara Alvarez, Committee Member Professor of Biomedical Engineering, NJIT	Date
Dr. Xin Di, Committee Member Research Professor of Biomedical Engineering, NJIT	Date
Dr. Hai Sun, Committee Member Associate Professor of Neurosurgery, Rutgers, New Brunswick	Date
Dr. William Graves, Committee Member Associate Professor of Psychology, Rutgers, Newark	Date
Dr. Sridhar Kannurpatti, Committee Member Assistant Professor of Radiology, Rutgers, Newark	Date

BIOGRAPHICAL SKETCH

Author: Rakibul Hafiz

Degree: Doctor of Philosophy

Date: May 2022

Undergraduate and Graduate Education:

- Doctor of Philosophy in Biomedical Engineering,
  New Jersey Institute of Technology, Newark, NJ, 2022

- Master of Science in Biomedical Engineering,
  New Jersey Institute of Technology, Newark, NJ, 2017

- Bachelor of Science in Electrical and Electronic Engineering,
  American International University Bangladesh, Dhaka, Bangladesh, 2012

Major: Biomedical Engineering

Presentations and Publications:

Hafiz, R., Gandhi, T. K., Mishra, S., Prasad, A., Mahajan, V., Di, X., Natelson, B. H. & Biswal, B. B. (2022). Higher limbic and basal ganglia volumes in surviving COVID-negative patients and the relations to fatigue. Neuroimage: Reports, 2(2), 100095. doi:https://doi.org/10.1016/j.ynirp.2022.100095

Hafiz, R., Gandhi, T. K., Mishra, S., Prasad, A., Mahajan, V., Di, X., Natelson, B. H. & Biswal, B. B. (2022). Assessing functional connectivity differences and work-related fatigue in surviving COVID-negative patients. *BioRxiv*, Epub 2022/02/09. doi: 10.1101/2022.02.01.478677. PubMed PMID: 35132408; PMCID: PMC8820653 interests.

Chen, D. Y., Ji, K. C., Varshney, S., Hafiz, R., Biswal, B. B. (2021). Chapter 4 - Resting state functional connectivity in pediatric populations. In: Huang H, Roberts TPL, editors. Advances in Magnetic Resonance Technology and Applications; Cambridge, Massachusetts: Academic Press; p. 65-87.

Ionescu, T. M., Amend, M., Hafiz, R., Biswal, B. B., Maurer, A., Pichler, B. J., Herfert, K. (2021). Striatal and prefrontal D2R and SERT distributions contrastingly correlate with default-mode connectivity. *Neuroimage*, 243, 118501. doi:https://doi.org/10.1016/j.neuroimage.2021.118501

Ionescu, T. M., Amend, M., Hafiz, R., Biswal, B. B., Wehrl, H. F., Herfert, K., Pichler, B. J. (2021). Elucidating the complementarity of resting-state networks derived from dynamic [18F]FDG and hemodynamic fluctuations using simultaneous small-animal PET/MRI. *NeuroImage,* 236, 118045. doi:https://doi.org/10.1016/j.neuroimage.2021.118045.

To my daughter… my Northern Star, my life, and the fuel to my endeavors. My love for you is without end …

To my wife… the immovable rock and the love of my life, the ray of hope and glue that holds everything together. My world would collapse without you, but the 'knot' keeps growing stronger everyday with your boundless love and support.

To my mother-in-law… or 'momma' as my daughter calls her, none of us could ever repay you for everything you did to look after our daughter. You are a true blessing from above. Thanks for being the best grandmother to Wardaa and cooking all the delicious meals every day.

To my late father-in-law… We can never forget your tremendous support and cheer during our days of struggle and being the best grandfather to Wardaa. May you rest in peace.

And finally…
To my parents… the source of my existence, my two superheroes. The two most important people who taught me to be kind, generous and honest, against all odds, the epitome of compassion and patience. If I could even be 1% of a father to Wardaa as you have been to me, 'Abbu' (father), I would consider myself blessed and fortunate. 'Ammu', my dearest mother, no amount of achievement in my life can outweigh the tears you have shed in prayers for me. My life and everything in it, belong to you and 'Abbu'.

"To be nobody but yourself,

in a world which is doing its best, night and day,

to make you everybody else –

means to fight the hardest battle which any human can fight;

and never stop fighting."

– E. E. Cummings

ACKNOWLEDGMENT

I would like to sincerely thank my advisor Dr. Bharat B. Biswal for his tremendous support throughout the entire process of this project's completion and facilitating the collaboration with the Indian Institute of Technology (IIT) team. My sincerest gratitude goes to the co-advisor Dr. Xiaobo Li, for her support and valuable insights.

My gratitude also to my committee members Drs. Xin Di, Tara Alvarez, Hai Sun, William Graves and Sridhar Kannurpatti, who indicated critical points and provided relevant insights that helped improve this project significantly.

Thanks to the Department of Biomedical Engineering (BME) at NJIT for their financial support. I would also like to thank the National Institutes of Health (NIH, grant R01AT009829) for their research funding.

Huge thanks to Dr. Tapan K. Gandhi and Sapna Mishra from the IIT team who did the hard work of recruiting COVID patients and providing the imaging data.

A huge thanks to Drs. Mesut Sahin and Alev Erdi for the administrative support and coordinating the program-related process.

Lastly, I am very grateful to my colleagues at the NJIT Brain Connectivity Lab – Donna, Wonboom and Alexandros for being a great support. I am very proud and glad to work with such a hard-working team.

TABLE OF CONTENTS

TABLE OF CONTENTS
(Continued)

Chapter **Page**

TABLE OF CONTENTS
(Continued)

TABLE OF CONTENTS
(Continued)

Chapter **Page**

LIST OF TABLES

LIST OF FIGURES

LIST OF FIGURES
(Continued)

Figure **Page**

LIST OF FIGURES
(Continued)

Figure **Page**

LIST OF FIGURES
(Continued)

Figure **Page**

LIST OF FIGURES
(Continued)

Figure **Page**

LIST OF SYMBOLS

©	Copyright
Δ	Delta (change in a variable)
χ^2	Chi-Squared (statistical test)
Z	Z-score (standardized score)
ρ	rho (Spearman's Correlation)
r	Pearson's Correlation
$\approx$	Approximately

LIST OF DEFINITIONS

Morphometry	Changes in brain structure due to natural development, injury or neurodegeneration.
Functional Connectivity	Statistical dependency between two variables across time.
Resting State	A state of data acquisition when a participant remains at complete rest keeping movements to minimum.
Independent Component Analysis	An algorithm that decomposes the brain into distinct networks based on temporal similarity.
PASC	A recent condition among COVID survivors experiencing persistent symptoms, also known as post-acute sequelae of SARS-CoV-2 infection or 'long-COVID'
Hyposmia	A symptom among COVID patients experiencing reduced or loss of sense of smell.
Framewise Displacement	A method to assess in-scanner head movement frame by frame.
FWE Correction	A correction method for multiple comparisons that controls for the family-wise-error-rate.
Pre-Processing	A set of steps used to clean or purify the brain imaging data to remove unwanted noise or nuisance signals.

CHAPTER 1

INTRODUCTION

1.1 Objective

At the early stage of the COVID-19 pandemic, the medical communities put a significant amount of effort towards acute patients, focusing primarily on dealing with the respiratory damage done by the novel coronavirus. Understandably at that time, the primary target was saving lives of critical patients and as a result, a large portion of survivors who got discharged from the hospital remained neurologically uninvestigated. Some of the recovery stage symptoms experienced by these survivors over long term, tend to be cognitive in nature, therefore, the brain might play a considerable role in mediating them. Our objective was to study the brain at an early stage of recovery (2 weeks after discharge) by applying structural and functional neuroimaging in COVID survivors and comparing them with a group of healthy controls (HCs). Furthermore, we wanted to evaluate how these brain estimates correlate to self-reported fatigue levels during work.

Multiple cerebro-vascular injuries have been found in acute COVID patients (Gulko et al., 2020). This can lead to changes in structural properties in the brain which can be estimated using T1-weighted magnetic resonance imaging (MRI) imaging. Similarly, damages in neurons and vasculature can also lead to local changes in metabolic activity which can be estimated using functional MRI (fMRI). Interestingly loss/reduction in sense of smell (hyposmia) is highly prevalent among COVID survivors (Logue et al., 2021; National Center for Immunization and Respiratory

Diseases (NCIRD), 2020; Peluso et al., 2021). How such brain alterations differ particularly in the COVID subtypes (hyposmic and non-hyposmic), and the healthy groups need to be investigated. This led to two broader research questions – do brain abnormalities persist in PCR negative survivors at an earlier point of recovery, particularly, two weeks after hospital discharge? Moreover, is work-related fatigue correlated to brain estimates in these groups?

Based on recent neuroimaging evidence, we hypothesized that brain structure and function will be altered across these three groups and their brain estimates will demonstrate a significant relationship with work-related fatigue. Therefore, we performed T1-weighted high resolution structural MRI and resting state functional MRI (RS-fMRI) to obtain brain structural and functionality metrics in the three groups to test the two hypotheses. This has been laid out in three specific aims and briefly summarized, as follows –

1. Assess alterations in gray matter volume using voxel-based morphometry (VBM) in hyposmic, non-hyposmic and healthy subjects.

   1.a Here, we quantified gray matter volume (GMV) using VBM and used a one-way analysis of variance (ANOVA) to first delineate global changes in GMV. We then performed a voxelwise search across the whole brain to identify brain regions with significant differences in GMV across the three groups in specific clusters obtained by a non-stationary cluster extent threshold.

   1.b Post-hoc tests were then performed on those specific clusters to evaluate differences in GMV across each group pair.

2. Estimate functional brain changes in hyposmic, non-hyposmic and healthy subjects.

   2.a Local brain activity was estimated using amplitude of low frequency fluctuations (ALFF). One way ANOVA was performed voxelwise to identify brain regions with altered activity across the three groups.

2.b Group level functional connectivity (FC), was estimated using independent component analysis (ICA) to identify distinct resting state networks (RSNs), followed by dual regression to obtain subject specific maps. Statistical analysis was performed to show differences between groups for specific RSNs.

3. Evaluate the relationship of fatigue with structural and functional brain estimates across hyposmic, non-hyposmic and healthy subjects.

   3.a Fatigue scores from all three groups was used in a single multiple linear regression model to assess correlation with GMV. The individual effects of each group that drove the overall trend was assessed to show which group was more susceptible to fatigue.

   3.b The same regression analysis was performed for the functional brain metrics: ALFF and FC of RSNs to assess functional correlates of fatigue in these groups.

CHAPTER 2

NEUROLOGICAL DAMAGE AND HYPOSMIA IN COVID-19

In Chapter 1, the overall objective of this study was presented. The research questions leading to the specific hypotheses were discussed. Furthermore, the three specific aims and the sub-aims designed to test the hypotheses of the study were also laid out. In this chapter, we briefly introduce COVID-19 in general and the development of cases that led to evidence of neurological signatures in COVID survivors. We also summarize the studies relevant to the research questions based on the most recent literature review.

2.1 Background

SARS-CoV-2 (Severe Acute Respiratory Syndrome Coronavirus 2) is a highly contagious novel coronavirus that primarily uses respiratory droplets as a medium to spread rapidly across humans (National Center for Immunization and Respiratory Diseases (NCIRD), 2020). As of February 2022, the number of confirmed cases have reached over 400 million, with nearly 6 million deaths around the world ((WHO), 2022). The alarming rate at which the virus spreads from person-to-person has delayed scientific investigations to understand and strategize against its attack on major biological systems (Puntmann et al., 2020; Zhao et al., 2020; Zubair et al., 2020). With the rapid production of vaccines, strict mask mandates and social distancing, the spread and severity of the viral attack have been mitigated significantly. However, the novel coronavirus has also evolved in a short time and the wave of new strains such as the ‘delta’ and ‘omicron’ variants have affected densely populated countries more severely, India, being a prime example.

The devastation led by the initial attack and the delta wave had almost paralyzed India. Due to a large influx of patients, supplies were depleting quickly, adding on to other complications. As a result, the primary interest was to save lives of critical patients with respiratory failure or severe damage to the respiratory system and to be fair, such was the case across most countries in the world. This led to a vast majority of hospital survivors whose brain alterations were not studied. With time, studies have begun to emerge identifying symptoms that last from a few weeks to several months after initial infection (del Rio et al., 2020; Logue et al., 2021). Importantly, three recent cohort studies point to the brain as one of the primary organs responsible for these symptoms: one such surveying 177 patients up to 9 months after infection reported fatigue (13.6%) and loss in sense of smell (13.6%) as the most common symptoms (Logue et al., 2021); a second reported fatigue (92%), concentration and memory loss (74%), weakness (68%), headache (65%) and dizziness (64%) (Tabacof et al., 2020); and a third following 179 COVID patients (Peluso et al., 2021) at least 6.5 months after acute COVID infection noted fatigue, shortness of breath, concentration problems, headaches, trouble sleeping and anosmia/dysgeusia.

Based on input data collected from 4 million patients across US, Sweden and UK, a recent article for primary care clinicians has classified subjects with symptoms lasting beyond 12 weeks as 'chronic' COVID-19 (Greenhalgh et al., 2020). The National Institutes of Health (NIH) have made a high priority of studies of this new condition and called it 'post-acute sequelae SARS-CoV-2 infection (PASC)'. Because the most common symptoms of the PASC patient (and of chronic fatigue syndrome or CFS) are fatigue and cognitive complaints and the most common sign is neurological – hyposmia or anosmia,

our initial hypothesis is that the brain is responsible for the survivors to experience these symptoms. What we do not know is whether there are any early recovery stage neurological manifestations (e.g., 2 weeks after hospital discharge) in the hospitalized survivors? Do these neurological alterations also relate to behavior, such as, work-related fatigue? This is exactly what we intend to investigate in this study.

2.2 Neurological Damage in COVID Survivors

If the brain plays a role modulating some of the symptoms that develop both during and after initial infection (PASC), then neuroimaging studies can non-invasively investigate where these alterations manifest (cross-sectionally) and develop over time (longitudinally). Early neurological investigations involving severely ill COVID patients have shown some evidence on the attack on the central nervous system (CNS). Increased cytokine levels have been found to play a crucial role in compromising the immune system in COVID-19 patients (H. Li et al., 2020). A study consisting of eight severely ill patients showed that, serum from a single patient had elevated levels of IL (interleukin)-6 (Keller et al., 2020) suggesting that cytokines or inflammatory processes causing metabolic changes that transfer from peripheral blood to the CNS may be responsible for disturbances in the blood-brain barrier and dysfunction in brain tissue. MRI of intracranial vessel wall revealed contrast enhancement of mid-to-large sized cerebral arteries which can be the cause of several inflammatory vascular pathologies (in 25% of patients) (Keller et al., 2020). Similar vascular abnormalities were reported from a single center from 4 COVID patients (Nicholson et al., 2020). A review consisting of twenty-two articles covering 5 investigational studies, 6 case series, and 11 case reports on 126 patients from seven

different countries, report that brain MRI revealed acute infarct, posterior reversible encephalopathy syndrome, cortical fluid-attenuated inversion recovery (FLAIR) signal abnormality and microhemorrhages (Gulko et al., 2020).

Kremer et al., 2020 conducted a retrospective study on data collected over multiple centers (11 hospitals, n = 64). They report several neurological aberrations including high percentage ischemic strokes (27%) and encephalitis (13%, more common in younger patients) (Kremer et al., 2020). Structural MRI imaging showed abnormalities in 56% of the cohort. Irregularities in mental capabilities are also reported with highest cases of confusion (53%), impaired consciousness (39%) along with agitation (31%) and headaches (16%). They also report hyperintense brain regions from FLAIR and white matter (WM) abnormalities from diffusion weighted images (DWI) observed from individual patients. Another multicenter study found neurological alterations in 50 out of 235 ICU patients with severe COVID-19 symptoms (Kandemirli et al., 2020). They report hyperintensity observed from FLAIR MRI images in all major brain lobes in specific patients. Similar results were also reported in another study with 29 COVID-19 positive patients in individual patient's FLAIR images (Paterson et al., 2020). Another study (Helms et al., 2020) also reported frontotemporal hypoperfusion observed in all (n = 11) COVID patients who underwent MRI, most likely because of hypoxia induced from acute respiratory distress syndrome (ARDS) associated with COVID-19. Additionally, olfactory dysfunction or loss of sense of smell (hyposmia or anosmia) is also commonly reported among acute and PASC patients. The next section expands on the neurophysiology and current neuroimaging findings of olfactory dysfunction among COVID survivors, since the current study emphasizes on this subtype.

2.3 Olfactory Dysfunction in COVID Survivors

Although the pathophysiology of how the novel coronavirus enters the brain and attacks the CNS is still under investigation, interestingly, its predecessors have been shown to travel across nerve synapses and attack the CNS (Dubé et al., 2018; Li et al., 2013). It is still unclear whether SARS-CoV-2 enters the brain using the same pathways, but previous reports in mice suggest that SARS-CoV-1 (immediate predecessor of SARS-CoV-2) invades the brain via a transcribrial route (Matsuda et al., 2004; McCray et al., 2007). This suggests that the virus enters the brain through the cribriform plate and then attacks the olfactory cortex producing pathology which can be detected with neuroimaging tools. To cite a few single patient reports in support of this statement: two MRI studies done on two acutely ill patients (age 27, male and age 25, female) showed bilateral olfactory edema with severe enlargement and abnormally high intensity (Laurendon et al., 2020) and hyperintense FLAIR uptakes (Politi et al., 2020). Abnormalities reported from these studies suggest possible structural and functional alterations in the olfactory system. But do these effects exist or persist in survivors? If so, how are the effects in the hyposmic group different from the non-hyposmic and healthy groups?

Some evidence of altered neurophysiology among hyposmic/anosmic patients exist both from single case and cohort specific reports in the literature. The two studies cited in the previous paragraph (Laurendon et al., 2020; Politi et al., 2020) were among the early reports suggesting olfactory dysfunction. The first case of anosmia associated with COVID-19 in Taiwan was reported from a male patient, who demonstrated hyperintensity in the olfactory bulbs (C.-W. Li et al., 2020). Similar findings were also reported from a single patient (age 25, Female) with hyperintensity in the gyrus rectus, olfactory bulbs

which returned to normal when scanned again on day 28 (Politi et al., 2020). Asymmetry in olfactory bulb was also observed in postmortem study of 4 deceased COVID-19 patients (Coolen et al., 2020). A recent study (Esposito et al., 2022) has shown abnormally higher structural and functional connectivity in the hyposmic group (n = 27) compared to normosmic group (n = 18). Several brain regions with functional connections to the piriform cortex were compromised and more segregated in the hyposmic group. In a more clinical setting, another study (Niesen et al., 2021) investigated six patients with positron emission tomography and MRI (PET-MR) and showed blockage within the olfactory cleft. The patient sample in this study was unique in the sense that they had lost their sense of smell 'suddenly' and they make an interesting case that this is not a direct result of a neuroinvasive attack by SARS-CoV-2, rather, a residual effect of other related physiological processes in the olfactory system initiated by the virus.

Indeed, the effects discussed so far need to be replicated over a larger sample and across different sites for reliability. Further investigation is also necessary to delineate the neuro-physiological processes in hyposmic, non-hyposmic and healthy subjects. Neuroimaging techniques provide an opportunity to assess this non-invasively. Our goal is to leverage this and systematically evaluate brain alterations in these groups using structural and functional neuroimaging metrics.

CHAPTER 3

STRUCTURAL ALTERATIONS IN COVID SURVIVORS

Chapter 2 broadly presented evidence of CNS attack by the novel coronavirus and depicted the neurophysiology of olfactory dysfunction. This chapter will focus on highlighting how structural alterations differ among hyposmic, non-hyposmic and healthy subjects. This chapter is addresses specific aim 1 and the sub-aims, which were laid out in Chapter 1. First, current findings in the literature are presented to provide the basis behind the hypothesis being tested in aim 1. Then, the method and analysis pertaining to the morphometry analysis is presented in sequence. Finally, the most relevant results are highlighted and discussed.

3.1 Introduction

3.1.1 Background

Most early COVID neuroimaging studies have investigated structural modulation among severely ill patients. Brain lesions, detected using FLAIR imaging, have been reported within frontal, parietal, occipital, temporal, and insular lobes (Kandemirli et al., 2020). Another study investigating three COVID patients with autoimmune and hemorrhagic encephalitis reported abnormal uptake on FLAIR imaging within the hypothalamus, temporal lobe, and the thalamus (Paterson et al., 2020). But these were mostly case studies, and investigators acknowledged the necessity to move from individual cases to cohort specific group effects. This helps in delineating structural brain alterations between COVID-19 survivors and healthy controls (HCs) with higher statistical power.

To address this gap in knowledge, a few neuroimaging studies have emerged with moderate (Duan et al., 2021; Qin et al., 2021) to large sample sizes (Douaud et al., 2021), including follow-up (Lu et al., 2020; Tu et al., 2021) and longitudinal designs (Douaud et al., 2021). Lu et al., 2020 (Lu et al., 2020) found neurological symptoms in over 68% (41/60) of hospitalized patients and after a 3 month-follow-up, reported persisting neurological symptoms in 55% (33/60) of patients. They had also used MRI imaging to assess both gray matter volume (GMV) and white matter (WM) structural alterations. They further showed significantly higher GMV in several regions of interest (ROIs) – Rolandic operculum, bilateral olfactory, insular, and hippocampal regions, as well as in the right cingulate gyrus and left Heschl's gyrus. Another study with follow ups after 3 and 6 months showed increased GMV in bilateral hippocampus and amygdala (Tu et al., 2021).

The effects could also be due to symptomatic severity such as fever or hypoxemic conditions. Such conditions can modulate the brain structure that could relate to clinical measures more locally despite no significant changes in GMV overall. For instance, a recent study has used Computed Tomography (CT) scans to show that the fronto-temporal network is more susceptible to fever and reduced oxygen levels in COVID patients, despite no overall difference in GMV between the COVID and control groups (Duan et al., 2021). There have also been cases, where the patients never showed any neurological manifestations in the acute stage. The question remains whether they can develop neurological symptoms during recovery. In that case, how are these developments different in mild and severe patients? A recent study has addressed this with two sub-types (mild and severe) who had no signs of any neurological manifestations during the acute stage

(Qin et al., 2021). However, after a 3 month-follow-up MRI scan, they reported reduced cortical thickness in the left insula, hippocampus, and superior temporal gyrus.

How the neurophysiological changes develop in individuals before and after infection with COVID-19 can also reveal critical information on the progressive atrophy in brain structure. The UK Biobank COVID-19 reimaging study is among the first longitudinal studies to address this, leveraging a large sample of patients (N=785, n_{COVID} = 401) (Douaud et al., 2021). They show reduced GM thickness and contrast in the orbitofrontal and parahippocampal gyrus, as well as, in insula, amygdala and the anterior cingulate cortex. In addition, they report increased tissue damage in brain regions functionally associated with the piriform cortex and the olfactory system, as well as higher volumes in CSF. Interestingly, the mixed evidence of increased GMV and contrarily, reduced GM thickness from these studies, reveal brain alterations in otherwise quite consistent anatomical locations. Our goal was to first assess, if the participants from this study, scanned after a much shorter interval from hospital discharge (2 weeks), demonstrated altered GMV in regions that are consistent with both acute stage single case reports and more recent group level neuroimaging reports from lengthy recovering (3 to 6 months) patients.

In the current study, we address this by recruiting a group of patients, hospitalized after a positive PCR test for COVID-19 with multiple symptoms. This group of patients was further divided into sub-types based on those who experienced a loss of sense of smell (hyposmic, also referred as 'LOS' group in this study) and those that did 'not' experience a loss of sense of smell (non-hyposmic, also referred as 'nLOS' group in this study). They were imaged two weeks after hospital discharge after converting to be PCR negative. One

expectation is that changes in brain tissue structure in COVID survivors can still cause changes in compartmental volumes that remain shortly after hospital discharge. Specifically, we hypothesized that the hyposmic (LOS) group would demonstrate gray matter volume (GMV) differences with the non-hyposmic (nLOS) and HC group. T1-weighted MRI images can be utilized to estimate GMV differences between the groups using voxel-based morphometry (VBM) (Ashburner & Friston, 2000).

VBM is a volumetric computational method that can quantify voxel-wise changes in tissue volume in the gray matter (GM)(Ashburner & Friston, 2000). It is a useful method to report group level differences in tissue volume between patients and healthy controls (HCs), using T1-weighted anatomical images. Its application in patient cohorts is quite popular with earliest reports for schizophrenia (Wright et al., 1999; Wright et al., 1995), autism (Abell et al., 1999), chronic depression (Shah et al., 1998) and epilepsy (Woermann et al., 1999) among several others (Krams et al., 1999; May et al., 1999; Vargha-Khadem et al., 1998). More recent reviews on VBM application across different neurological diseases can also be found, e.g., for schizophrenia (Nemoto, 2017), autism spectrum disorder (Yamasue, 2017), epilepsy (Yasuda et al., 2010) and Alzheimer's disease (Matsuda, 2016).

3.2 Materials and Method

3.2.1 Participants

The on-site team from the Indian Institute of Technology (IIT), Delhi, India, recruited 47 COVID-negative patients and 35 HCs, where they were imaged following the Institutional Review Board (IRB) guidelines. All patients are local inhabitants of Delhi, India, who were

recruited from a much larger pool of patients. The patients were initially classified by the Metro Heart and Super-specialty Hospital, New Delhi, India based on illness severity data derived from a database of 2,538 COVID patients from May to December 2020. 24% of this sample did not require O_2, 40% required O_2, 22% required Continuous Positive Airway Pressure (CPAP); and 14% were intubated. This 14% of intubated patients were excluded from the recruitment process in the current study.

Of the remaining patients, 333 needed CPAP to raise O_2 levels; 333 needed nasal O2 to raise O_2 levels; and 334 were admitted but did not need supplemental O_2. The sample of 47 COVID subjects constituting the COVID group in this study were collected from this cohort (those who agreed to participate in this ongoing study so far). Patients were studied two weeks after discharge, after becoming PCR negative. Any subject from the healthy group who has experienced fever, cough, or flue like symptoms in the two weeks prior to scan or from past medical records based on self-report, were removed from the study. All healthy subjects also had to undergo a PCR test to prove that they had not been infected in the recent past. We used a questionnaire to record symptoms the survivors have experienced during hospitalization (see Figure 3.1) and an additional questionnaire to quantify fatigue levels (see Figure 3.2) which also included similar questions from the first questionnaire to identify if they experienced any persistent or new symptoms.

To avoid confounding effects from comorbidities, we recruited subjects that were, otherwise, in excellent health conditions prior to hospitalization for COVID-19. For example, 16/47 (34.04%) of our patients were young adults who had no prior record of any comorbidities that could confound the COVID-19 effects. We only had 7/47 (14.89%) subjects with age between 50-54 years (capped at < 55 years as recruitment criteria to avoid

other comorbidities), some of whom had reported to have marginal diabetes. The rest (51.07%) in between also did not have any record of comorbidities from the hospital.

Table 3.1 summarizes the clinical information from the 47 patients included in the current study. It shows percentages of patients in each category of symptom severity, medications administered and requiring additional oxygen support. Of these 47, 36.17% (17/47) patients were reported to be 'mild', 8.51% (4/47) to be 'moderate' and 36.17% (17/47) to be 'severe'. Information from the rest of the 19.15% (9/47) was not provided from the hospital because those patients did not give consent to sharing their medical symptoms. Please note, we present percentages of affected patients as a ratio of both the available sample with information ('% Out of Avail.' in Table 3.1) and the total sample of patients including those patients who did not give consent to share their clinical data ('% Out of Total' in Table 3.1). Among the severe patients, 58.82% (10/17) were given Remdesivir and 29.41% (5/17) required additional oxygenation. One patient (1/17) was given a mix of Dexamethasone, Ceftriaxone and Clexane injections and another (1/17) was put in an Antibiotic and Steroid regime for 4 weeks (Progressively reduced). One other patient (1/17) was given Actemra 2 times, who was also administered Bilevel Positive Air Pressure (BiPap) for 4-5 days. On average these 47 patients stayed in the hospital for approximately 11 ± 3.30[SD] days.

Before data analysis, six subjects (1 COVID and 5 HC) were removed during quality control assessment. The quality control step involved a visual assessment and it included – identifying subjects with major injuries in the brain, images without full brain coverage, abnormal segmentation and normalization and artifacts in the image among others. Effectively, T1-weighted images from 46 (31 males) COVID and 30 (23 males)

HCs were included in the study with mean age 33.5 years ± 9.74[SD] years (HC) and 34.63 years ±11.54[SD] years (COVID). Please see Table 3.2 for more details on demographics. The most reported symptoms from the participants during hospitalization were - fever, cough, body ache, chills, difficulty breathing, bowel irritation, nausea, loss of sense of smell and loss of consciousness.

3.2.2 Clinical Assessment

The most frequently observed symptoms from the participants during hospitalization were - fever, cough, body ache, chills, difficulty in breathing, bowel irritation, nausea, loss of sense of smell and taste and loss of consciousness. From the day of discharge till the day of scan, we asked if the participants were experiencing any persistent or new symptoms. Work-related fatigue (86.84%), muscle pain (18.42%), lack of sleep (39.47%), lack of attention (36.84%), headache (36.84%), joint pain (50%), memory loss (34.21%), delayed recovery of sense of smell (44.74%) and/or taste (34.21%), bowel irritation (57.89%) and interestingly, hair loss (81.58%) were commonly reported. Please note, most survivors experienced multiple symptoms simultaneously, hence the '%' represents symptoms that overlap within participants. For example, 36.84% of 27 post-COVID participants reporting with lack of attention also reported a work-related fatigue score > 2, with 'work-related fatigue' pointing exclusively to their daily professional work. A point to note here is that fatigue was the highest reported symptom in this cohort (> 86% of COVID participants), which is a sign of cognitive decline, and this adds on to the rationale behind particularly investigating this symptom exclusively.

Name: _____ **Date of Birth:** _____

Age: _____ **Sex:** _____ **Date of Scan:** _____

Instructions: Please read the following questions carefully and answer them accurately. It is vital for our study to assess the progress of your COVID history (should you have/had been diagnosed). If you have any concerns about any question, please do not hesitate to ask the investigator for a clarification. Please answer with tick marks and put dates in the format MM/DD/YYYY where applicable. If a question is not applicable to you, tick the ☐ N/A.

1.	Do you currently have/had (past) any symptoms related to COVID-19?	☐ Yes	☐ No	☐ N/A
2.	What date did the symptoms start?	/ /		☐ N/A
3.	What date did the symptoms stop?	/ /		☐ N/A
4.	What date did you get tested?	/ /		☐ N/A
5.	Did your symptom include fever?	☐ Yes	☐ No	☐ N/A
6.	Did you have chills?	☐ Yes	☐ No	☐ N/A
7.	Did you have cough?	☐ Yes	☐ No	☐ N/A
8.	Did you have body ache?	☐ Yes	☐ No	☐ N/A
9.	Did you have diarrhea?	☐ Yes	☐ No	☐ N/A
10.	Did you have difficulty breathing?	☐ Yes	☐ No	☐ N/A
11.	Did you have bowel irritation?	☐ Yes	☐ No	☐ N/A
12.	Did you have nausea?	☐ Yes	☐ No	☐ N/A
13.	Did you lose your sense of smell?	☐ Yes	☐ No	☐ N/A
14.	If yes to Q13, what date did you start losing your sense of smell?	/ /		☐ N/A
15.	If yes to Q13, what date did you regain your sense of smell?	/ /		☐ N/A
16.	Did you lose your sense of taste?	☐ Yes	☐ No	☐ N/A
17.	If yes to Q16, what date did you start losing your sense of taste?	/ /		☐ N/A
18.	If yes to Q16, what date did you regain your sense of taste?	/ /		☐ N/A
19.	Did you lose consciousness?	☐ Yes	☐ No	☐ N/A
20.	If you tested negative upon retesting, do you have any persistent symptom?	☐ Yes	☐ No	☐ N/A

Figure 3.1 Participant recruitment questionnaire for symptoms during hospitalization. The figure shows the list of questions the participants were requested to answer to evaluate the development and duration of specific symptoms relating to COVID-19 during hospitalization.

3.2.3 MRI Imaging

A 3T GE scanner was used to acquire high-resolution T1-weighted images. The subjects were placed in a supine position and asked to remain still. The images were acquired using

a 32-channel head coil in 3D imaging mode with a fast BRAVO sequence. Imaging parameters include inversion time, TI = 450 ms; 244 x 200 matrix; flip angle = 12° and field of view, FOV = 256 mm, slice thickness of 1.00 mm and spatial resolution of 1.0 mm x 1.0 mm x 1.0 mm. The whole brain was scanned in the sagittal configuration to collect 152 slices. Raw Digital Imaging and Communications in Medicine (DICOM) images were reconstructed into Neuroimaging Informatics Technology Initiative (NIfTI) format for data curation, pre-processing and sub-sequent analyses performed.

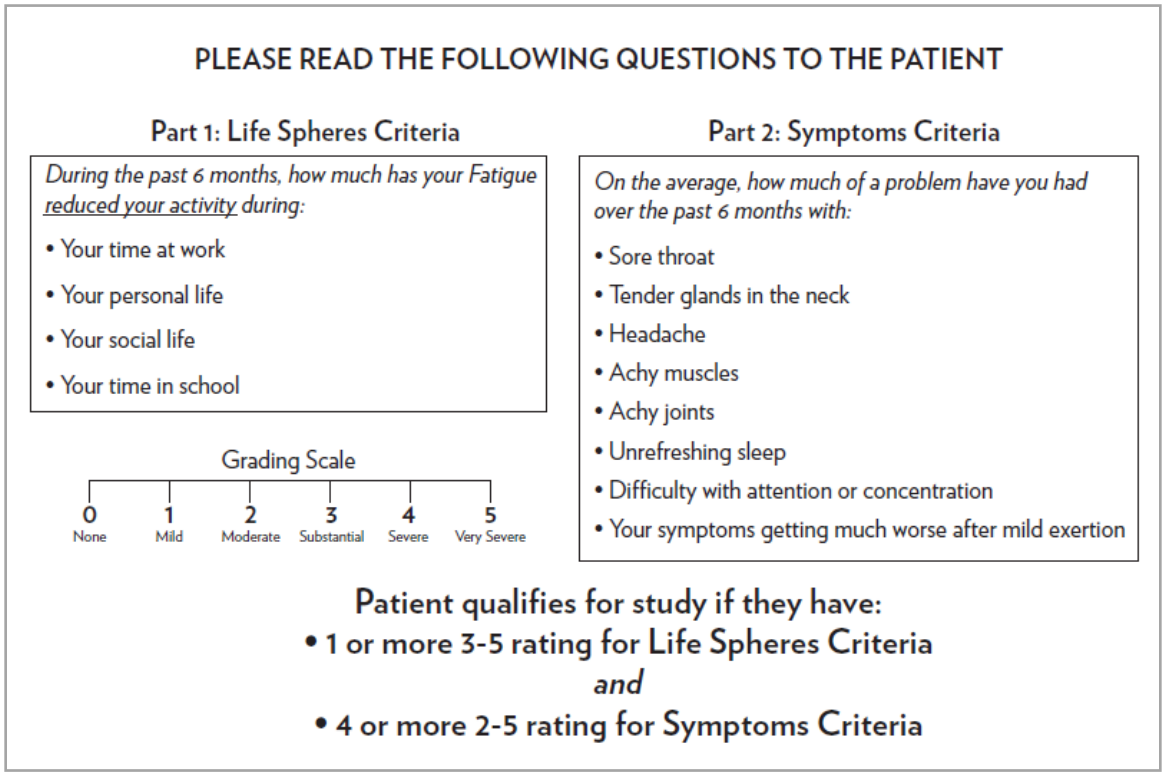

Figure 3.2 Fatigue and long-COVID related symptoms questionnaire. The 'Part 1' on the left is the fatigue questionnaire based on 'Life Spheres Criteria' shown in the bullet points. The participants were asked to grade their fatigue levels on a scale of 0-5 with increasing fatigue severity as the number approaches 5. A secondary, 'Part 2: Symptoms Criteria' questionnaire (on the right) was also provided to the surviving patients. This was done to identify persistent or new symptoms possibly relating to PASC development. We were particularly focused on the fatigue levels experienced during work and all results and evaluations are reported based on the fatigue scores at work.

Source: Natelson, B. H. (2019). Myalgic Encephalomyelitis/Chronic Fatigue Syndrome and Fibromyalgia: Definitions, Similarities, and Differences. Clinical Therapeutics, 41(4), 612-618. https://doi.org/https://doi.org/10.1016/j.clinthera.2018.12.016

3.2.4 Image Pre-Processing

'Pre-processing' is a term typically associated with MRI and fMRI data. This entails a number of steps incorporated to condition the imaging data and remove unwanted noise and unrelated sources that may obscure the true effects. It is also important because without these steps, false positive results can be introduced during the statistical analysis. Since this chapter highlights estimates derived from anatomical MRI, only the pre-processing steps involved with this modality is depicted. In effect, the pre-processing steps described below is a sub-set of functional MRI data pre-processing, as it also relies on high resolution anatomical images for registration and spatial interpretation purposes. More information on functional imaging data pre-processing can be found in Chapter 4.

SPM12 (http://www.fil.ion.ucl.ac.uk/spm/) was primarily used for pre-processing the anatomical data. Custom scripts within the MATLAB environment (MathWorks Inc, Massachusetts, USA) were prepared to perform pre-processing on T1w MRI images. All anatomical images were visually inspected for artifacts, re-centered and reoriented to the anterior-posterior commissure (ac-pc) line. Each brain compartment was segmented into specific tissue classes mainly - gray matter (GM), white matter (WM), and cerebro-spinal fluid (CSF). A study-specific template was first generated using the fast diffeomorphic image registration algorithm (DARTEL) (Ashburner, 2007) which is representative of the average across all the participants included in the study (Ashburner & Friston, 2009; Yassa & Stark, 2009). Subject level maps were non-linearly warped to this reference template for relatively higher specificity and accuracy (Yassa & Stark, 2009). Finally, each map was normalized to the Montreal Neurological Institute (MNI) space using affine transformation and resampled to an isotropic voxel dimension of 1.5 mm x 1.5 mm x 1.5 mm. Modulated

images were obtained for each subject, which account for contractions and expansions from non-linear spatial transformations. The normalized modulated images were then spatially smoothed with a gaussian kernel of 8 mm. This increases the signal to noise ratio (SNR) by suppressing the noise in the image and reducing the inhomogeneities across neighboring voxels. The final output of this step from each subject was then used in subsequent statistical analysis.

Table 3.1 Clinical Assessment of COVID Patients

Clinical Assessment	No. Aff.	No Info.	Data Avail.	No. Tot.	% Out of Avail.	% Out of Total
Symptom Severity						
Mild	17	9	38	47	44.74	36.17
Moderate	4	9	38	47	10.53	8.51
Moderate-Severe	17	9	38	47	44.74	36.17
Medications & Support						
Remdesivir	10	9	38	47	26.32	21.28
Additional O_2	5	9	38	47	13.16	10.64
BiPap & Actemra	1	9	38	47	2.63	2.13
Mix Medications*	1	9	38	47	2.63	2.13
Antibiotic & Steroid	1	9	38	47	2.63	2.13

Keys: No. Aff. = number of affected patients, No Info. = no information available because these patients did not give consent to share symptom information, Data Avail. = number of subjects with clinical assessment data available, No. Tot. = total number of patients including those with no information available, % Out of Avail. = proportion of patients affected vs patients with clinical assessment data available (n = 38) in percentages, % Out of Total = proportion of patients affected vs. total number of patients (n = 47) in percentages, O_2 = oxygen supplied to support breathing, BiPap = bilevel positive air pressure, Mix Medications* = a combination of medications – Dexamethasone, Ceftriaxone and Clexane injections

Table 3.2 Summary Statistics of Participant Demographics and Global VBM Metrics

Dem. / G.VBM	Score (*test*), *p value*	HC mean (SD)	nLOS mean (SD)	LOS mean (SD)
Age (years)	-0.93 *(F)* 0.399	33.50 (9.74)	36.13 (12.17)	31.81 (10.02)
Sex† (M/F)	1.04 *(χ^2)* 0.59	23M 7F	21M 9F	10M 6F
Fatigue (0-5)	22.07 (χ^2) 1.61e-05 **	0.65 (0.79)	2.89 (1.18)	2.40 (1.35)
GMV (ml)	3.48 *(F)* 0.036 *	629.59 (44.17)	620.76 (65.63)	671.18 (86.09)
WMV (ml)	1.95 *(F)* 0.95	394.44 (42.51)	408.80 (44.97)	420.47 (40.14)
CSFV (ml)	1.01 *(F)* 0.37	246.49 (59.72)	259.70 (52.19)	270.55 (58.34)
TIV (ml)	3.09 *(F)* 0.05	1270.52 (106.92)	1281.27 (127.78)	1362.20 (147.87)

Keys: Dem. = participant demographics (first three rows), G.VBM = global VBM metrics (last four rows), HC = healthy control group, nLOS = no loss of smell (non-hyposmic) group, LOS = loss of smell (hyposmic) group, mean = mean across group, SD = standard deviation, Sex† = only frequency of male (M) and female (F) shown for the categorical variable 'sex' instead of mean and SD, *F* = *F-statistic* from ANOVA, χ^2 = *chi-squared* test on 'sex' and *Kruskal-Wallis* test on 'Fatigue', ** = significant with $p < 0.001$, * = significant with $p < 0.05$, GMV = gray matter volume, WMV = white matter volume, CSFV = cerebrospinal fluid volume, TIV = total intracranial volume and ml = milliliter.

3.2.5 Voxel Based Morphometry (VBM)

VBM can be estimated from gray matter probability maps obtained from the 'segmentation' stage of pre-processing described in Section 3.2.4. Each value in a tissue specific probability map represents the likelihood or probability of the voxel belonging to a brain compartment. By compartments, we primarily refer to three major tissues comprising the brain, namely, the gray matter (GM), white matter (WM) and cerebro spinal

fluid (CSF). The tissue volumes of a specific compartment can be estimated by summing over the product of each voxel's dimension and the corresponding probabilities (Lüders et al., 2002). The volumes of each major compartment can be summed over to generate a global quantity of a specific brain called, the total intracranial volume (TIV).

The compartmental volumes reported in this study are labelled as gray matter volume (GMV), white matter volume (WMV), and cerebro-spinal fluid volume (CSFV). These quantities were used to assess central tendency measures in each group. It should be noted that only the GMV is eventually used in the voxelwise analysis as this is the brain compartment of primary interest. To visualize the sample distributions and group average compartmental and total brain volumes, we customized and adopted a script in RStudio (RStudio, 2021) to generate a 'raincloud' figure, as depicted in a recent publication (Allen et al., 2021).

3.2.6 Statistical Analysis

Once pre-processing was performed and VBM was estimated for each voxel within the GM, the next step was to analyze the data to identify any difference across the group. But an important prior step is to assess the participant demographics and make sure there were no differences being driven by factors like age and sex. These variables were controlled for in all brain metric analyses. To assess differences in participant demographics across groups, we performed a one-way ANOVA on age and a chi-squared test for differences in proportion of males and females (sex) across the three groups.

Fatigue is a central quantitative variable of interest in our study. We also first assessed if there is any differences in fatigue across these three groups. For all parametric tests, we performed prior assumption tests involving deviation from normality and

homogeneity of variance. To test for deviations from normality, *Shapiro-Wilk* tests were performed to check if any p-value was less than 0.05. Deviation from homogeneity of variance was checked with *Levene's* test and similarly, p-value less than 0.05 was assessed. Particularly, the fatigue scores deviated from normality (*Shapiro-Wilk,* $p < 0.05$). Therefore, we used Kruskal-Wallis test across groups and post-hoc Wilcoxon's ranksum test to assess difference between group pairs among HCs and COVID subjects.

We also performed a one-way ANOVA on global VBM metrics including GMV, WMV, CSFV and TIV. The results from all these tests are summarized into a data table, as shown in Table 3.2. The statistical tests depicted thus far, help with inference on global metrics. To obtain more localized effects, voxelwise analysis was performed and regions with significant effects across group was identified.

To determine group level differences in GMV at a voxel level, we performed a one-way ANOVA using the smoothed, modulated, and normalized GM tissue maps from the three groups. TIV of each subject was group-mean centered and added as a covariate along with age and sex to account for confounding effects. An implicit mask with absolute threshold of 20% above the group mean was set to exclude unwanted voxel quantities from the smoothed GM maps. In order to reduce multiple testing and only focus on relevant regions, the *F*-statistic map was conservatively thresholded at $F > 9$ $(p < 0.001)$, and regions with significant difference in GMV across groups were identified using a non-stationary cluster-based correction at a cluster extent threshold of 533 voxels and adjusted for multiple comparisons with *family wise error (FWE)* correction at $p_{FWE} < 0.05$. The average GMV from these significant clusters was then extracted and a multiple linear regression analysis was performed using age, sex and TIV as covariates of no interest. The

mean across groups was then added back to the residuals and eventually post-hoc *two-sample t-tests* were performed on these metrics to identify GMV differences between HC, Hyposmic (LOS) and non-Hyposmic (nLOS) groups.

3.2.7 Visualization and Plotting

While statistical tests help making group level inferences, the main effects often get eclipsed by statistical thresholds such as t or F scores. While these scores are important, they are however, arbitrary and do not have units. Therefore, it is also important to assess the main effects through central tendency metrics. It is also important to look at the probability distributions that drive such effects. In order to keep all these effects intact, 'raincloud' figures were generated, as depicted in a recent publication (Allen et al., 2021).

The central tendency measures of GMV, WMV, CSF and TIV in each group was assessed and visualized using probability distributions and group average compartmental and total brain volumes. The purpose of computing central tendency measures was to visualize the probability distributions of the global volume metrics. While we only performed group level statistics on the GMV, assessing the central tendency measures also helps us appreciate the other tissue volumes in the two groups including WMV, CSFV and TIV. A customized script was generated from a package in RStudio (RStudio, 2021) to generate the raincloud figures. A similar method was also adopted to obtain a different variation of raincloud plots in MATLAB (MathWorks Inc, Massachusetts, USA) and show the distribution, dot and box plots within the same figure for better visual aesthetics. These figures help capturing the group differences in the significant clusters in a more 'statistically' intuitive way by preserving each group's main effects.

3.3 Results

3.3.1 Participant Demographics and Global Metrics

In this section, we will report results from the demographics and global VBM metrics, as these tests were performed prior to voxel-wise analysis. The 'global VBM metrics' is meant to refer to the entire compartmental volumes for GM, WM and CSF, as well as the whole brain (TIV). Table 3.2 summarizes the results from the statistical tests on participant demographics (age, sex and fatigue) across each group, as well as global metrics including GMV, WMV, CSFV and TIV from the VBM analysis. The first three rows in the table summarizes the participant demographics. No significant differences were observed in age and sex across groups ($p > 0.05$). On the other hand, a *Kruskal-Wallis* test on fatigue scores (Table 3.2, 3rd row) revealed a significant effect ($p = 1.61e\text{-}05$) across the three groups. Post-hoc *Wilcoxon Ranksum tests* further revealed that the fatigue scores in the HC group were significantly lower compared to both nLOS ($p = 1.12e\text{-}05, T = 175.50$) and LOS ($p = 5.11e\text{-}04, T = 191$) groups. This demonstrates that fatigue levels observed among HC group is significantly lower than the COVID group in general. No significant difference was observed between the fatigue scores of nLOS and LOS groups. This indicates that the level of fatigue experienced by the hyposmic (LOS) and non-hyposmic (nLOS) groups is similar during daily work.

Rows 4-7 in Table 3.2 summarizes the results from the global metrics computed from the VBM analysis. There was a significant difference in overall GMV across the groups ($p = 0.036, df = (2,73), F = 3.48$). Post-hoc two-sample *t*-tests with Bonferroni correction showed that the difference in overall GMV was between LOS and nLOS groups ($t = 2.38, df = 44, p = 0.036$). The significant results from the demographics (fatigue) and

VBM global metrics (GMV) are presented with statistical results and corresponding 'raincloud' plots in Figure 3.1. The figure shows estimated probability distributions, box plot with interquartile range and jittered dot plots representing individual participant values. This helps in not only interpreting the group level differences, but also appreciate the differences in main effects of across groups. Figure 3.1 (A) shows a significant gap in distributions between nLOS and HC and LOS and HC groups which is reflected in summarized statistics depicted in the previous paragraph. Similarly, Figure 3.1 (B) shows that the overall GMV of the LOS group was higher compared to nLOS group (significant at $p < 0.05$) and HC group (not significant as $p > 0.05$).

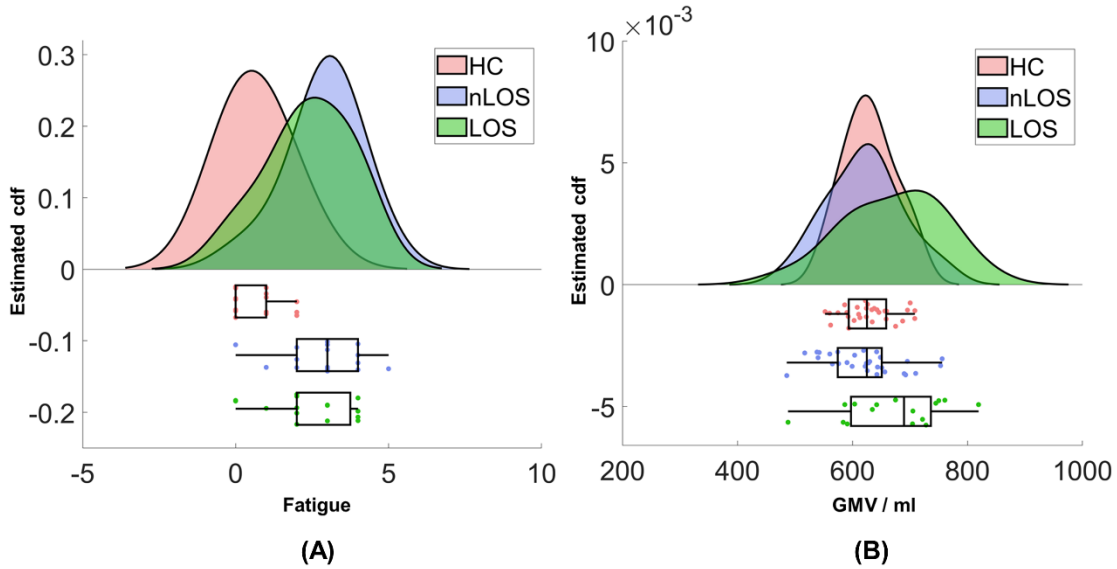

Figure 3.3 'Raincloud' plots from the significant results from statistical analysis on participant demographics and global VBM metrics. The light pink represents the HC group, light purple the nLOS group and lime green the LOS group, respectively. The area plots (top) represents an estimated probability distribution plot from the data. The box and dot plots (bottom) represents interquartile range and individual participant data that reflects on the distribution plots above. (A) Higher fatigue levels observed in nLOS and LOS groups compared to HCs. This is apparent from the shift in the distribution plots to the right from both nLOS and LOS groups. Since the nLOS and LOS plots follow closely, no difference was observed between these groups. (B) Higher GMV observed in the LOS group compared to nLOS group. A shift in overall GMV distribution of the green plot (LOS) to the right is clearly observed. Keys: cdf = cumulative distribution function ml = milliliter.

3.3.2 Voxelwise VBM

In this section, the results from the voxelwise analysis will be presented focusing only on the GMV alterations. The voxelwise analysis helps to identify exactly which locations in the brain these abnormalities exist across groups. Figure 3.2 shows the results from the voxelwise one-way-ANOVA analysis, indicating, a difference in GMV across the three groups. Particularly, four clusters survived *family-wise error correction (FWE)* for multiple comparisons at a non-stationary cluster threshold of $k_E = 533$ voxels. The clusters comprised of bilateral brain regions that are constituents of the *limbic system*, *occipitotemporal* and *cerebellar* lobes. The cluster details and relevant statistical parameters have been tabulated in Table 3.3. The anatomical regions listed in Table 3.3 were identified based on data as provided by Neuromorphometrics, Inc (Neuromorphometrics) embedded within SPM.

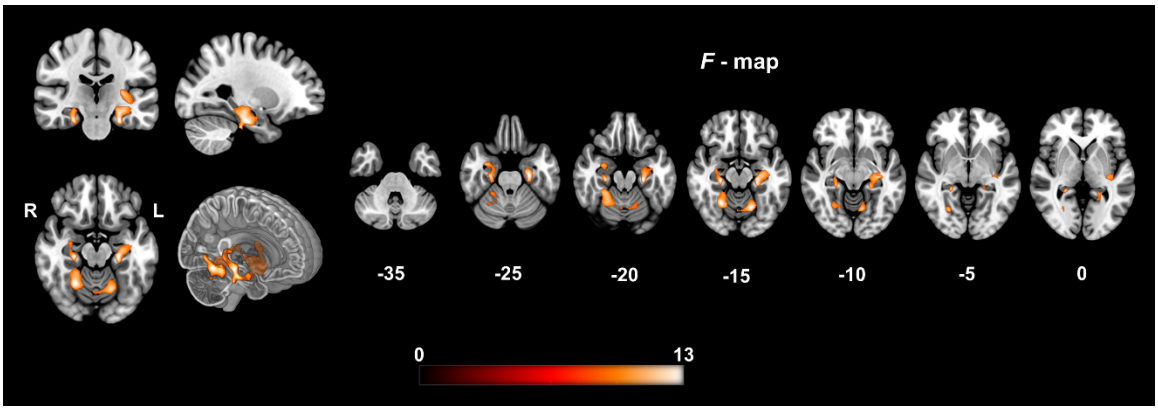

Figure 3.4 Voxelwise one-way ANOVA reveals significant differences in GMV across groups. The figure on the left shows four significant clusters in three orthogonal planes and a cut-to-depth volume rendered image for better interpretation of the spatial locations the clusters comprise of. The multi-slice axial view on the right shows the spatial extent of these clusters in finer slices (*Z-slices = -35:5:0*). More specifically, the clusters were majorly centered within *bilateral hippocampal* and *parahippocampal* gyri from the *limbic system*, *exterior cerebellum* and *vermal lobules* within the *cerebellar* lobe and *lingual* and *fusiform* gyri from the *occipitotemporal* lobe. The colorbar represents *F-statistic* values. The cluster peaks were located at MNI coordinates: [-24 -26 -20], [-15 -62 -14], [20 -40 6] and [24 -56 -16]. The peak *F-scores* and corresponding *FWE* corrected p-values were: F_{peak} = [14.08, 13.74, 13.48, 13.31] and p_{FWE} = [0.0002, 0.035, 0.001, 0.012], respectively.

The results and tabulations in Figure 3.2 and Table 3.3 suggest that the GMV is altered across the three groups. However, it does not delineate which direction the differences exist. This was achieved by running post-hoc *two-sample t-tests* across pairs of groups. As mentioned in Section 3.2.5, to avoid multiple testing the post-hoc tests were performed only on the four significant clusters observed from the ANOVA analysis. Figure 3.3 shows the binary masks of each cluster that were used to obtain the average GMV for all subjects in each group. A raincloud plot is also paired with each cluster's binary map which shows the estimated probability distributions and corresponding dot and box plots. These plots help identifying which group distribution was more shifted compared to others, causing GMV differences between specific groups.

The post-hoc tests from cluster 1 revealed that GMV in the LOS group was significantly higher compared to both HC (*t = 5.91, df = 44, p = 4.65e-07;* where *t = two sample t-test statistic, df = degrees of freedom* and *p = p-value*) and nLOS (*t = 5.63, df = 44, p = 1.19e-06*) groups. However, no significant difference in GMV was observed between HC and nLOS group ($p > 0.05$). This is also reflected in the raincloud plot of cluster 1 in Figure 3.3 (*top left*). The green distribution plot belongs to the LOS group, and it is shifted more to the right suggesting higher GMV in this group compared to the light pink and light purple plots representing HC and nLOS groups, respectively. The box plot with the green dots shows that the median in LOS group was more shifted to the right compared to the other groups, again, indicating higher GMV in this group. It can also be noted that the HC and nLOS plots follow each other closely and therefore no GMV differences were observed between these two groups.

Table 3.3 Cluster Information from Voxelwise ANOVA on GMV

Cl. No.	Left / Right	Anatomical Regions (Neuromorphometrics)	Peak MNI Co. X	Y	Z	Cl. Size	Peak F, (p_{FWE})
1	*Left*	*Parahippocampal Gyrus (PHG)*	-24	-26	-20	1580	14.08 (0.0002)
		Hippocampus (Hc)					
		Fusiform Gyrus (FuG)					
		Planum Polare (PP)					
		Posterior Insula (PIns)					
2	*Left*	*Cerebellum Exterior (CExt.)*	-15	-62	-14	533	13.74 (0.035)
		Lingual Gyrus (LiG)					
		Cerebellar Vermal Lobules (CVL) I-V					
		Cerebellar Vermal Lobules (CVL) VI-VII					
3	*Right*	*Parahippocampal Gyrus (PHG)*	20	-40	6	907	13.48 (0.001)
		Hippocampus (Hc)					
		Posterior Cingulate Gyrus (PCgG)					
		Fusiform Gyrus (FuG)					
		Thalamus Proper					
4	*Right*	*Cerebellum Exterior (CExt.)*	24	-56	-16	1220	13.31 (0.012)
		Lingual Gyrus (LiG)					
		Fusiform Gyrus (FuG)					

Keys: Cl. No. = cluster number, Left/Right = left or right hemisphere of the brain, MNI = Montreal Neurological Institute, Co. = coordinates, X Y Z = x, y and z MNI coordinates in mm, Cl. Size = cluster size in voxels, Peak F = peak voxel *F-statistic* value in x, y and z MNI coordinates, p_{FWE} = *FWE* corrected exact p-value after multiple comparison correction.

Similarly, for cluster 2, the LOS group demonstrated higher GMV compared to both HC (*t = 4.96, df = 44, p = 1.11e-05*) and nLOS (*t = 4.67, df = 44, p = 2.81e-05*) groups. This is also reflected on the raincloud plot shown in Figure 3.3 for cluster 2 (*top right*). The results from the two clusters presented in the top row of Figure 3.3 comprised

of brain regions from the left hemisphere. For cluster 1, the anatomical regions included the *limbic system (PHG, Hc)*. For cluster 2, the anatomical regions were primarily from the *cerebellar* lobe (*CExt*).

The bottom row of Figure 3.3 shows map-plot pairs from clusters 3 and 4, respectively. Post-hoc tests on cluster 3, revealed that LOS group had higher GMV compared to both HC (*t = 5.56, df = 44, p = 1.48e-06*) and nLOS (*t = 4.88, df = 44, p = 1.43e-05*) groups within the *right PHG* and *Hc* from the *limbic system*. This can also be quite clearly followed from the raincloud plots in Figure 3.3 for cluster 3 (*bottom left*). Finally, cluster 4 comprised of *right occipitotemporal* and *cerebellar* brain regions (*FuG, CExt*) where, the LOS group demonstrated higher GMV compared to HC (*t = 4.97, df = 44, p = 1.05e-05*) and nLOS (*t = 5.01, df = 44, p = 9.33e-06*) groups. A familiar trend of the green distribution plot shifting right can also be observed from the raincloud plot in Figure 3.3 (*bottom right*). To summarize, GMV was higher in all four clusters in the LOS group compared to both HC and nLOS, indicating GMV alterations in the hyposmic group.

3.4 Discussion

The statistical results from the global morphometry metrics, particularly, GMV and voxelwise VBM analysis on GMV support our hypothesis that COVID survivors, now PCR negative, demonstrate altered GMV compared to HCs even 2 weeks after hospital discharge. Our results align with what is known from single case reports and group level effects available in the current literature. In this section, we expand on these findings and compare our results to interpret the results scientifically.

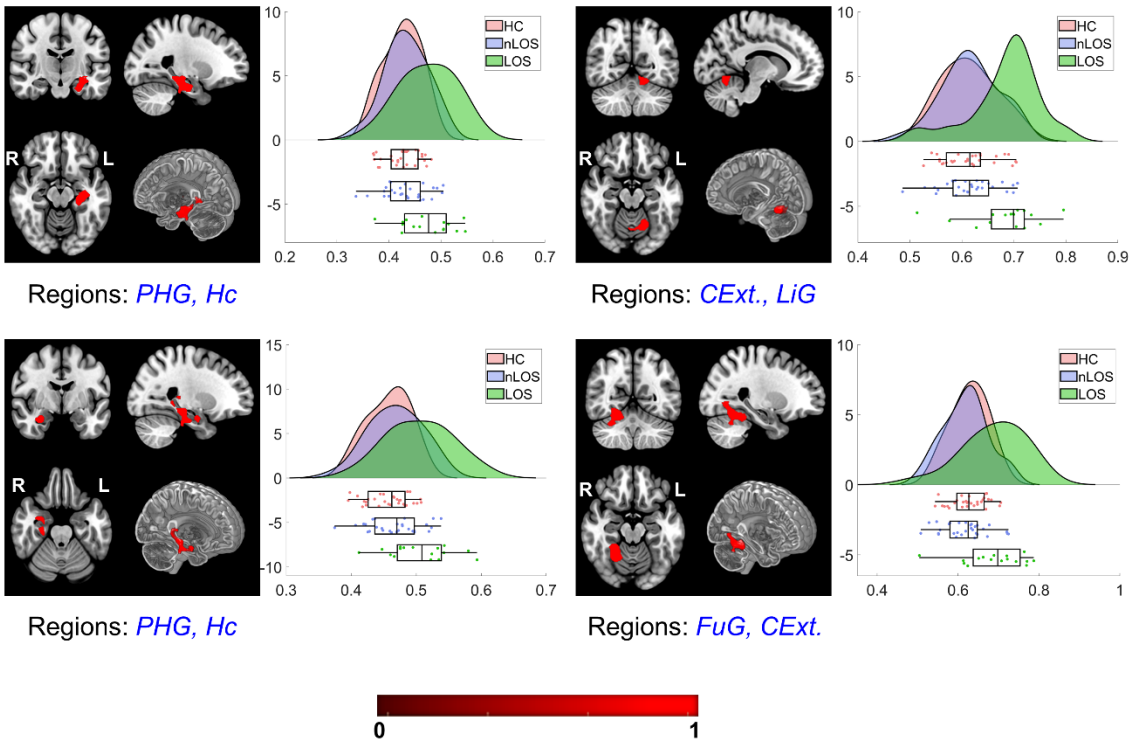

Figure 3.5 Binary map and raincloud plot pairs of the four major clusters from the one-way ANOVA analysis on which post-hoc tests were performed. The top row shows clusters from the left hemisphere and the bottom row shows the clusters from the right hemisphere. Cluster 1 is shown on the *top left*, which majorly comprised of *PHG* and *Hc*. This binary mask was used to obtain the average GMV within the cluster. The average GMV of all subjects from each group was then used to generate the raincloud plot right next to it. Similarly, pairs of binary map and raincloud plot are shown for cluster 2 (*top right*) comprising of *CExt* and *LiG*, cluster 3 (*bottom left*) of *PHG* and *Hc* and finally, for cluster 4 (*bottom right*) consisting of *FuG* and *CExt*. The colorbar shows range of values between 0 – 1 as the cluster maps shown are binarized and all red voxels have a value of 1. In the raincloud plots, the y-axis represents the estimated probability distribution values, and the x-axis represents the average GMV. The dot and box plots represents individual subject data and the interquartile range from each group.

3.4.1 Demographics and Fatigue in COVID Survivors

There was no significant differences in 'age' and 'sex' across the groups. We did our best to make sure the participant recruitment criteria already control for these demographics. It can be noted that the number of male participants was higher in the HC group. This was also true for the COVID group (NLOS and LOS). Therefore, we did not also observe any

difference in 'sex' across groups, nevertheless, the effects of 'age' and 'sex' were regressed out in all statistical analyses to remove any confounding effects.

We observed that the level of 'fatigue' experienced by the non-hyposmic (nLOS) and hyposmic (LOS) groups was higher compared to the HC group. On the other hand, within the COVID subtypes, i.e., nLOS and LOS groups experienced similar levels of fatigue (see Figure 3.1 (A) and Table 3.2). This clearly indicates that the COVID group was more susceptible to fatigue during work compared to the HC group. What we do not know, is how the brain derived quantities from structural and functional imaging relate to fatigue and exactly where these effects are exhibited in the brain. We address these gaps in our third aim and more information on the brain correlates of fatigue can be found in Chapter 5.

3.4.2 Higher Global VBM Metrics in Hyposmic Group

We observed higher overall compartmental GMV in the hyposmic (LOS) group compared to nLOS and HC groups ($p < 0.05$). Although not statistically significant ($p > 0.05$), it is interesting to note that the mean compartmental CSFV tended to be higher in the LOS group compared to nLOS and HC group (see Table 3.2). This seems to align with the recent UK-Biobank longitudinal study (n = 401), who reported increased CSFV after COVID infection (Douaud et al., 2021). Our data indicates more variation in brain volumes among the LOS patients, with higher standard deviation (SD) in GMV (see Table 3.2). This might arise from varying levels of tissue swelling due to acute infection among surviving patients. More importantly, *olfactory* alterations from case reports suggest neuro-invasion can lead to GMV abnormalities in regions associated with the olfactory system and beyond. For example, edema in the bilateral olfactory lobes led to severe enlargement and abnormally

high FLAIR intensity in a single acute patient (Laurendon et al., 2020). Similarly, abnormal intensities in the *olfactory* lobe were also observed from a clinical patient from a different site (C.-W. Li et al., 2020) and hyperintensity in the *gyrus rectus* and *olfactory* bulbs were also observed in another study (Politi et al., 2020). Asymmetry in olfactory bulb was also observed in four dead COVID-19 patients (Coolen et al., 2020).

However, the underlying neurophysiology that elicit such changes is still unclear. Highly prevalent acute stage neurological damage from CNS viral or vascular pathologies can cause local changes in tissue concentration. Transient reduction in cerebral blood flow (CBF) can also cause gray matter volume to increase due to change in hydration levels (Ge et al., 2017). Overall, continued brain swelling from neuro-vascular injuries may explain why we observed globally higher GMV in the LOS group even 2 weeks after being PCR negative.

3.4.3 Group Level Differences Align with Hyperintense FLAIR Reports

The first neuroimaging (mostly MRI) studies involving COVID-19 were clinical case reports of acutely ill patients. Since our patient cohort was hospitalized during the acute stage, we first tried to observe if the brain regions with GMV abnormalities replicate the hyperintense brain regions in those early reports. We observed higher GMV in the LOS group bilaterally in the *left* and *right hippocampus* (*Hc)* compared to both nLOS and HC groups. This aligns with a case report of hyperintense *left Hc* from FLAIR images in an older patient (Male, 56 years) (Kremer et al., 2020). Hyperintensity in FLAIR images can arise from several sources including ischemia, micro-hemorrhages, and damage to vasculature, commonly observed in acute COVID patients and these neurological disturbances can modulate tissue volumes.

We also observed higher GMV in *posterior insula* (*PIns)* regions indicating GMV alterations in *insular* lobes, which were reported to be hyperintense in specific patients (Kandemirli et al., 2020). We found higher GMV in the LOS group within *lingual* and *fusiform gyri (LiG* and *FuG)* which are constituent of *occipito-temporal* lobes. This aligns with case reports from Kandemirli and colleagues (Kandemirli et al., 2020) who also found hyperintensities in the *occipital* and *temporal* lobes in specific patients. Similarly, hyperintensities were reported in the *temporal lobe* and the *thalamus* in individual patient's FLAIR images (Paterson et al., 2020). Our VBM results also show that the GMV within *planum polare (PP)* and *thalamus proper (ThP)* was higher in the LOS group. Higher GMV was also observed bilaterally in the *exterior* and several *vermal layers* within the *cerebellum.* A case report of a 47-year-old male described hyperintense *bilateral cerebellar hemisphere* and *cerebellar vermis,* which was also the first reported case of acute cerebellitis in COVID-19 (Fadakar et al., 2020). Another case of cerebellitis was also reported recently, adding on to the wide range of neurological disturbances in the CNS (Malayala et al., 2021). To summarize, our group level VBM analysis shows differences in GMV between LOS, nLOS and HC groups with higher GMV in brain regions that were found to be hyperintense in several acute patient reports.

3.4.4 Group Level Differences Align with Group Level Neuroimaging Reports

Recent neuroimaging studies have also reported higher GMV among COVID cohorts, in the *bilateral Hc* after 3 month-follow-up (Lu et al., 2020), as well as, in *bilateral Hc* and *Amg* in another follow-up study (3 and 6 months) (Tu et al., 2021). Interestingly, Tu et al., 2021 also report significant correlation of the *left Hc* and *Amg* with PCL-5 scores, demonstrating stress related structural changes in these regions. On the contrary, cortical

thickness was reported to be reduced in the *left Hc* after a 3 month-follow-up study (Qin et al., 2021) and in the *Amg* after infection with COVID-19 in a longitudinal study (Douaud et al., 2021).

Similarly, higher GMV was also observed at the group level in the *bilateral Ins* (Lu et al., 2020), while, on the other hand, others reported reduced cortical thickness in *insular* lobes (Douaud et al., 2021; Qin et al., 2021). To summarize, the group level estimates from our VBM analysis converge with clinical findings from acutely ill 'individual' COVID patients. The results are also consistent with current neuroimaging reports from moderate to large samples of recovering COVID survivors.

3.4.5 Conclusion

In conclusion, our results highlight both global and local GMV alterations among hyposmic and non-hyposmic COVID patients and HCs. We have shown that GMV is significantly altered in hyposmic patients compared to both non-hyposmic and HC groups, in multiple brain regions which are commonly found to be abnormal in single patient case studies, as well as several neuroimaging studies from surviving COVID-19 cohorts. More importantly, these regions are also known to be modulated by neuronal damage and characterized from functional neuroimaging relating to fatigue, pain, emotion, attention, and somatosensory processing (Bornhövd et al., 2002; Inagaki et al., 2012; Sergeeva et al., 2015; van Schouwenburg et al., 2015). These cognitive symptoms are also experienced by 'long-COVID' patients; therefore, these findings could suggest some early indications of PASC that manifest much later in the recovery process.

CHAPTER 4

FUNCTIONAL ALTERATIONS IN COVID SURVIVORS

Chapter 3 presented evidence of structural abnormalities and higher fatigue levels in COVID survivors. This chapter will focus on highlighting how functional brain metrics differ among hyposmic, non-hyposmic and healthy subjects. This chapter addresses specific aim 2, discussed in Chapter 1. Similar to Chapter 3, we first present current findings in the literature that helped with a-priori information for the hypothesis being tested in aim 2. Then, the method and analysis pertaining to local brain activity and functional connectivity analysis is presented in sequence. The results from both analyses are also sequentially presented and discussed.

4.1 Introduction

4.1.1 Background

At the beginning of the pandemic, neuroimaging studies have mostly focused on structural MRI imaging to report brain abnormalities in acutely ill COVID-19 patients. It is not clear whether functional abnormalities co-exist with structural alterations in patients who have survived the infection and have been discharged from the hospital. A few recent studies have emerged which attempted to address the structural/functional alterations. However, further investigations across different sites are necessary for more conclusive inference. In this section, we try to address these gaps, by investigating functional imaging data from COVID survivors, now PCR negative, and healthy subjects.

In Chapter 3, CNS involvement suggested by early pandemic MRI reports from acutely ill patients with a wide range of cerebrovascular abnormalities were presented (Gulko et al., 2020; Kandemirli et al., 2020; Keller et al., 2020; Nicholson et al., 2020; Paterson et al., 2020). These single-case reports played a vital role in informing and shaping recent studies with primary focus on group level structural differences in moderate (Duan et al., 2021; Qin et al., 2021) to large sample groups (Douaud et al., 2021). Naturally, the initial neuroimaging investigations were targeted to brain abnormalities in severe patients. Therefore, a large sample of hospitalized survivors were not investigated, especially those with persistent symptoms. This led to a rise in follow-up studies on a span of 3 to 6 months after initial infection (Lu et al., 2020; Tu et al., 2021) and longitudinal designs (Douaud et al., 2021) where structural abnormalities were investigated before and after the pandemic. We have recently shown gray matter volume differences in survivors after a shorter interval (2 weeks after hospital discharge), as well as a stronger relation between gray matter volume and self-reported fatigue at work in COVID participants (Hafiz, Gandhi, Mishra, Prasad, Mahajan, Di, et al., 2022) (in press). It is still unclear, though, if such structural abnormalities are also accompanied by functional brain alterations in COVID-19 survivors.

4.1.2 Functional Magnetic Resonance Imaging and Functional Connectivity

To identify functional brain alterations in COVID survivors, non-invasive functional brain imaging can be incorporated. A well-established imaging technique to detect brain function is functional magnetic resonance imaging (fMRI). fMRI captures 3-dimensional brain images across time, typically, using echo-planar sequences. This generates a time-series of brain signals that indirectly represents neuronal firing (Ogawa et al., 1990) due to some experimental condition imposed on the participant or from spontaneous fluctuations. The

response detected by fMRI is much slower than neuronal activity because it is convolved with hemodynamic processes, making fMRI sensitive to changes in blood oxygen level dependent (BOLD) signals (Ogawa et al., 1990). Cerebrovascular pathologies in hospitalized COVID patients can modulate blood flow and neural metabolism in the brain. This can lead to abnormal BOLD activity across brain regions, causing changes in temporal synchronization. Functional connectivity (FC) is a measure of how two or more brain regions are temporally synchronized (De Luca et al., 2006; Fox et al., 2005; Fox et al., 2006; Friston, 1994; Friston et al., 1993; Greicius et al., 2003). FC has been estimated across multiple modalities (Horwitz, 2003) but perhaps more popularly related to resting state fMRI (RS-fMRI).

4.1.3 Resting State Functional Magnetic Resonance Imaging

Resting state fMRI (RS-fMRI) studies derive information from spontaneous fluctuations of BOLD signals while the brain is metabolically and functionally active under resting state conditions (Glover, 2011). The earliest 'resting state' study was demonstrated by Biswal et al., in 1995 (Biswal et al., 1995) and subsequent studies have shown that spatially distinct regions that are temporally synchronized may share information with each other (Cole et al., 2010; De Luca et al., 2006; Fox et al., 2005; Fox et al., 2006; Greicius et al., 2003; Kalcher et al., 2012; Meier et al., 2012). RS-fMRI does not require the subjects to perform any active task. It places minimal constraint on the patient and eliminates task related confounds. Moreover, RS-fMRI scans provide the advantage of broader flexibility in investigating multiple brain regions and, the entire brain (Damoiseaux et al., 2006; Raichle & Mintun, 2006; Shulman et al., 2004).

In RS-fMRI, the synchrony of the unconstrained intrinsic functional activity between segregated brain regions can be assessed using functional connectivity (FC) measures (Biswal et al., 1995; Lowe et al., 1998). FC is a measure of how two or more brain regions are temporally synchronized (De Luca et al., 2006; Fox et al., 2005; Fox et al., 2006; Greicius et al., 2003). FC, measured between a pair of brain regions, is used to reliably extract the baseline functional networks (FNs) of the human brain. FN can be defined as a network of multiple functionally connected brain regions that show similar temporal activation patterns. These quantities can be estimated quite effectively using RS-fMRI imaging. Functional changes can occur across different networks among survivors, owing to a range of symptoms experienced during the recovery phase. Therefore, we applied a data driven approach to estimate FC differences between healthy controls (HCs) and surviving, now COVID-negative, patients using RS-fMRI.

4.1.4 Measures of Functional Connectivity

A popular voxel-wise method applied in RS-fMRI is investigating amplitude of low frequency fluctuations (ALFF) (Zang et al., 2007). Biswal and colleagues have previously shown that majority of the power in resting state fMRI signals is characterized by low frequency oscillations (Biswal et al., 1995). ALFF is a measure of the total power that lies within such low frequency bands. It is a data driven, functional segregation method that can quantify local activation at the voxel level. Local brain activation can be quantified using ALFF as depicted in (Zang et al., 2007). ALFF represents voxelwise ‘localized’ brain activity. Therefore, if there are local cerebro-vascular alterations in specific brain regions causing abnormal BOLD signal oscillations, change in ALFF can be representative of that difference between the two groups.

Among several methods to estimate functional connectivity, Independent Component Analysis (ICA) is a popular data driven technique that groups all voxels in the brain into distinct spatial networks based on the similarity of time courses (McKeown et al., 1998). The large-scale resting-state networks (RSNs) derived from ICA have been shown to have local and higher-level associative hierarchy (Yeo et al., 2011) and replicate highly reproducible activation maps across subjects (Smith et al., 2009). FC estimates from group ICA and dual regression (C.F. Beckmann, 2009; Filippini et al., 2009) can be used to test our hypothesis that surviving COVID-negative patients would demonstrate altered FC in RSNs comprising cortical regions where hyperintensities have been reported from single cases and group level differences identified from recent neuroimaging studies.

4.1.5 Current Literature Findings

Among the earliest pandemic literature, a task-based fMRI study reported loss in task activation in the orbito-frontal cortex (OFC) and strong BOLD activations in the piriform cortex (Ismail & Gad, 2021) from a single female (25 years) COVID patient with persistent olfactory dysfunction. They used a simple smell on/off block design task. A single case resting state fMRI (RS-fMRI) study from an unresponsive patient reported intact functional connectivity (FC) of the default mode network (DMN) (Fischer et al., 2020), which was a good prognosis for ultimate recovery. However, these studies were case reports, which leaves the question of whether there are generalizable group level functional brain alterations in COVID survivors.

To that end, a few studies have emerged that report various functional abnormalities among COVID survivors. For example, the initial case report from (Fischer et al., 2020) has now been followed up with a group level report with specific focus on severe patients

who were initially unresponsive but recovered completely and were able to return (Fischer et al., 2021) to pre-COVID level behaviorally. When they compared the functional connectivity of these unresponsive patients with healthy controls, they found significantly reduced default mode network (DMN) connectivity and reduction in inter-network connectivity between DMN and salience (SAL) networks. Another study investigating dynamic functional connectivity reported that COVID-19 survivors spent abnormally longer time in a specific brain state involving sensorimotor and visual networks, as well as cerebellar and sensorimotor networks (Fu et al., 2021).

Based on our structural analysis results and current literature findings, we focused on FC alterations primarily in four networks – the basal ganglia, precuneus and bilateral somatosensory networks. The Basal ganglia is a major hub for projections to and from the cortex and more importantly, it has direct neurological connections to the olfactory system (Amunts et al., 2005; Soudry et al., 2011). Precuneus is a major part of the DMN network, and the somatosensory networks are associated with multiple body related stimuli which could relate to symptoms experienced by survivors.

4.2 Materials and Methods

4.2.1 Participants

We have previously described the participant demographics information in detail within Section 3.2.1 of Chapter 3. Please also check Table 3.1 for more information on medications, additional O_2 support and Table 3.2 for statistical results from age, sex and fatigue. The current analysis was performed on the same set of subjects. Therefore, the same descriptions are not repeated here to avoid redundancy. Please note, the number of

participants effectively used in the final analysis is not the same as the VBM analysis. Additional quality control steps are required for functional data. This includes checking for misregistration between each participant's anatomical and functional data after coregistration, misalignment of the normalized functional files with MNI template and excessive head motion. 9 COVID and 4 HC subjects were removed during the quality control assessment, leaving with an effective sample of 38 (25 males) COVID and 31 (24 males) HC.

4.2.2 Anatomical Magnetic Resonance Imaging

Imaging was performed in the Centre for Advanced Research in Imaging, Neuroscience & Genomics (CARING), Mahajan Imaging, New Delhi, India. High-resolution T1-weighted images were acquired on a 3T GE scanner with a 32-channel head coil in 3D imaging mode with a fast BRAVO sequence. The imaging parameters were TI = 450 ms; 244 x 200 matrix; Flip angle = 12 and FOV = 256 mm. The subject was placed in a supine position and the whole brain was scanned in the sagittal configuration where 152 slices were collected, and each slice was 1.00 mm thick. The spatial resolution of all the anatomical scans was 1.0 mm x 1.0 mm x 1.0 mm.

4.2.3 Resting-State Functional Magnetic Resonance Imaging

A gradient echo planar imaging (EPI) was used to obtain 200 whole-brain functional volumes. The parameters were: TR = 2000 ms; TE = 30 ms; Flip angle = 90, 38 slices, matrix = 64x64; FOV = 240 x 240 mm^2; acquisition voxel size = 3.75 x 3.75 x 3 mm^3. The participant was requested to stay as still and motionless as possible with eyes fixed to a cross on an overhead screen.

4.2.4 Data Pre-Processing

The data preprocessing was performed primarily using Statistical Parametric Mapping 12 (SPM12) toolbox (http://www.fil.ion.ucl.ac.uk/spm/) within a MATLAB environment (The MathWorks, Inc., Natick, MA, USA). However, some steps utilized useful tools from FSL (FMRIB Analysis Group, Oxford, UK) and AFNI (http://afni.nimh.nih.gov/afni) (Cox, 1996) for housekeeping, visual inspection and quality control purposes. At the beginning, first five time points were excluded from each subject to account for magnetic stabilization. The functional images were motion corrected for head movement using a least squared approach and 6 parameters (rigid body) spatial transformation with respect to the mean image of the scan. The subjects with excessive head motion were identified using framewise displacement (FWD) (Power et al., 2012). Additionally, time frames with high FWD crossing a threshold of 0.5 mm (Power et al., 2012) were identified along with the previous and the next two frames and added as regressors (Yan et al., 2016) during temporal regression of nuisance signals. If more than 50% of the time series data were affected due to regression of high motion frames the participant was removed from the analysis. Moreover, any participant with the maximum framewise translation or rotation exceeding 2 mm was removed from further analysis. Anatomical image from each subject was 'co-registered' to the mean functional image obtained from the motion correction step. T1-weighted image from each subject was segmented into gray matter (GM), white matter (WM), and cerebrospinal fluid (CSF) tissue probability maps and an average template including all participants was generated using DARTEL (Ashburner, 2007). This template was used to spatially normalize all functional images to the MNI space and resampled to isotropic voxel size of 3 mm x 3 mm x 3 mm. Time series, from brain compartments with

high physiological noise signals such as, CSF and WM was extracted by thresholding the probability maps from the segmentation stage above the 99th percentile, and first 5 principial components were obtained using a COMPCOR based (Behzadi et al., 2007) principal component analysis (PCA) from both tissues. These 10 components along with Friston's 24- parameter model (6 head motion parameters + 6 previous time point motion parameters + 12 corresponding quadratic parameters) (Friston et al., 1996) and time frames with high FWD (> 0.5 mm) were added as regressors in a multiple linear regression model to remove unwanted signals voxel-wise. The residuals from the regression step were then bandpass filtered between 0.01 to 0.1 Hz and finally, spatial smoothing was performed using a Gaussian kernel of 6 mm full width at half maximum (FWHM).

4.2.5 Head Motion Assessment

We performed in-scanner head movement assessment using mean Framewise Displacement (FWD) based on the methods depicted in (Power et al., 2012). This was performed between the COVID (LOS + nLOS) and the HC groups. A two-tailed two-sample student's t-test revealed no significant differences in mean FWD between the two groups ($t = -1.57$, $p = 0.12$, $\alpha = 0.05$).

4.2.6 ALFF, ICA and Dual Regression

ALFF was quantified in a voxel-wise manner by applying methods depicted in (Zang et al., 2007). The total power within the typical resting state band: 0.01 – 0.1 Hz was computed by summing over the amplitudes after a Fourier decomposition of the functional data time series. The raw ALFF values were then standardized to z scores. This was achieved by first obtaining the global mean and standard deviation over the whole brain in each participant using a brain mask. This mean value was subtracted from the raw ALFF

values at each voxel and divided by the standard deviation. These standardized maps were then used in the group statistical analyses.

Group level resting state networks were obtained by applying the 'gica' option of the 'melodic' module from FSL toolbox (FMRIB Analysis Group, Oxford, UK). All subjects' 4D functional images after pre-processing were temporally concatenated into a 2D matrix of 'space' x 'time' as delineated in (C.F. Beckmann, 2009) and 25 spatial maps were obtained. Resting State Networks (RSNs) were identified by matching ICs with the 1000 functional connectome project maps (Biswal et al., 2010) using Dice's coefficient and spatial correlations obtained from AFNI's '3dMatch' program (Taylor & Saad, 2013). Further visual inspection was performed to make sure all network regions aligned with the functional network and ROIs depicted in (Altmann et al., 2015; Shirer et al., 2012). Dual regression (C.F. Beckmann, 2009; Filippini et al., 2009) was performed leveraging the standardized group ICA output from the 'melodic' step and applying it directly to the 'fsl-glm' module in FSL to obtain subject specific RSN maps. The subject specific network maps were standardized to Z-scores before consequently applying them in statistical analysis to infer group level estimates.

4.2.7 Statistical Analysis

To identify differences in ALFF across the three groups, a multiple linear regression model was used where age and sex were added as covariates of no interest and *F* and *t* statistics were obtained by setting proper contrast levels for each group. This way all statistical results were obtained from a single model. A similar approach was also applied to investigate FC differences across the three groups. Age and sex were also regressed out in this analysis. For both models, significant clusters were identified and main effect of

interest from the corresponding contrast maps representing the difference in mean beta scores from two groups were obtained by thresholding the *t*-score map values that survived the corrected threshold. Cluster-based thresholding was applied at height threshold of $p_{unc} < 0.01$, with *family wise error* (*FWE)* correction at $p_{FWE} < 0.05$ for multiple comparisons. The cluster extent threshold (k_E) obtained from this step was used to generate corrected statistical maps for the contrasts with significant effects. Please note, the statistical analysis on demographics is already detailed in Chapter 3. These steps are therefore not listed here to avoid repetition.

4.3 Results

4.3.1 Local Brain Activity Alterations in COVID Survivors

We observed higher local brain activity, represented by ALFF, in both LOS and nLOS groups when compared to HC group. Figure 4.1 shows the statistical maps and brain regions where ALFF was higher in these groups. The LOS group demonstrated higher ALFF (Figure 4.1, *Top row*) in regions from the *orbital gyrus – posterior orbital gyrus (POrG)* and *medial orbital gyrus (MOrG); limbic system – hippocampus (Hc), parahippocampal Gyrus (PHG)* and *amygdala (Amg); basal ganglia – pallidum (Pd), basal forebrain (BsF)* and *putamen (Pu);* and also, the *temporal lobe – entorhinal area (Ent)* and *temporal pole (TP).* Similarly, the nLOS group also demonstrated higher ALFF when compared to HC group, however, no difference in ALFF was observed between LOS and nLOS groups. Brain regions where the nLOS group demonstrated higher ALFF (Figure 4.1, *Bottom row*) include the *right basal ganglia – Putamen (Pu), Caudate (Cd), basal forebrain (BsF)* and *Pallidum (Pd);* and also the *limbic system – hippocampus (Hc),*

parahippocampal Gyrus (PHG) and *amygdala (Amg)*. Since three tests were performed between three possible group pairs, the alpha value was *Bonferroni* corrected at $\alpha = 0.017$ (0.05/3).

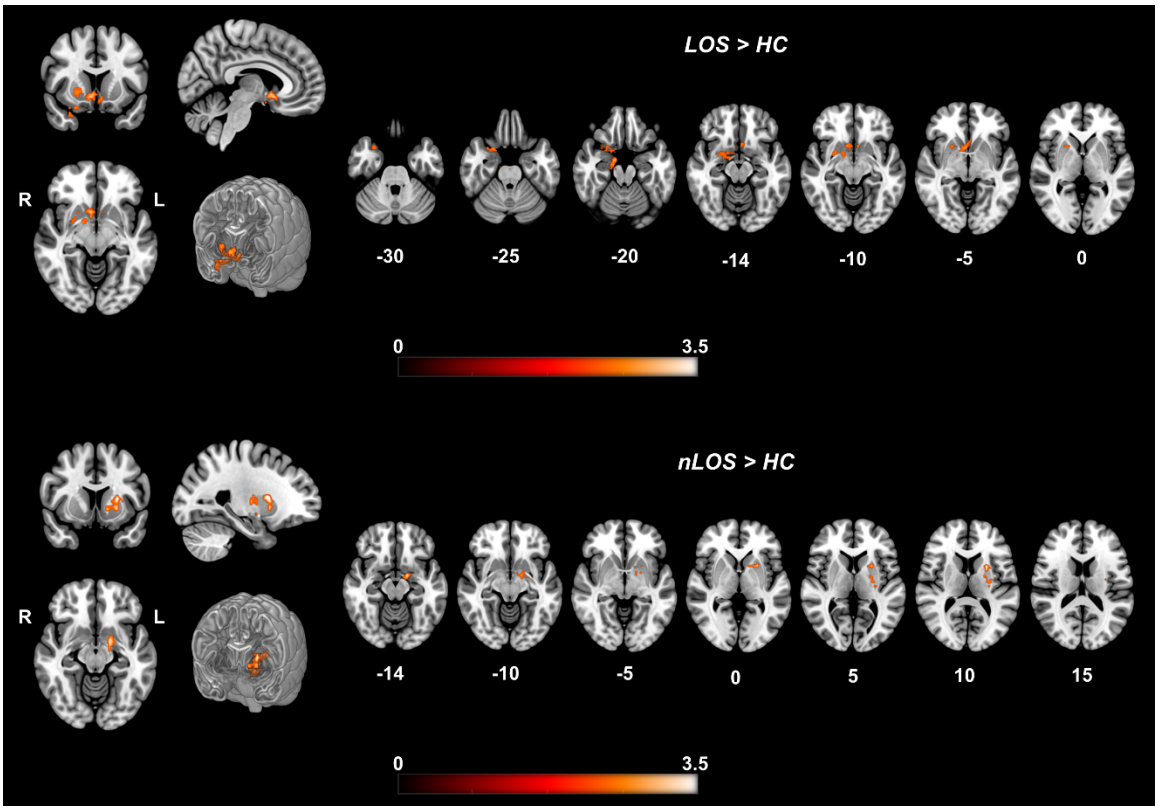

Figure 4.1 Higher ALFF observed in the COVID subtypes compared to HCs. (*Top row*) The three orthogonal slices and a volume rendered image on the left shows the cluster where ALFF was higher in the LOS group, comprising of regions from the *orbital gyrus*, *limbic system, basal ganglia* and *temporal lobe*. The cluster peak was observed at MNI coordinates: [21 9 -24] with peak *t-score* of T = 4.12, and corrected *p-value,* p_{FWE} = 0.00002. The cluster consisted of 147 voxels, and it was significant for a *Bonferroni* corrected *alpha value* of $\alpha = 0.017$. The colorbar shows *t-score* values. The multi-slice axial view on the right shows the cluster extent over finer Z slices. (*Bottom row*) Similarly, shows the cluster where nLOS group demonstrated higher ALFF compared to the HC group. The cluster was located in the left hemisphere, primarily comprising of regions from the *basal ganglia* and the *limbic system*. The cluster peak was observed at MNI coordinates: [-24 9 9] with peak *t-score* of T = 4.22, and corrected *p-value,* p_{FWE} = 0.001. The cluster consisted of 97 voxels, and it was significant for a *Bonferroni* corrected *alpha value* of $\alpha = 0.017$.

4.3.2 Functional Connectivity Alterations in COVID Survivors

From the group level ICA analysis, we identified twenty-two large-scale resting state networks (RSNs) (see Figure 4.2). These images represent group level RSNs from which subject level RSNs were obtained to run statistical analysis on specific networks. The maps represent standardized Z-scores which were thresholded at $Z > 3.3$, $p < 0.001$, to show robust functional connectivity in each network. The networks are presented in an orderly fashion based on their spatial location and functional characteristics. For example, the first row of images (Figure 4.2, top row) show networks involved primarily with visual (*MV1, LV,OCP, MV2*) and visuo-spatial (*DAN*) processing. Particularly, *PRN* is a relevant network to our hypothesis, as it is involved with a variety of complex cognitive functions.

From the second row, the *VDMN* and *PDMN* are primarily comprise the *default mode* networks and *RFP* and *LFP* constitute the *central executive* network associated with executive functions. *AUD*, *TPJN* and *LANG* (Figure 4.2, third row) are networks consisting of brain regions from the *temporal lobe,* involved in auditory, speech and language processing. *EXEC* from the third row in Figure 4.2 is associated with executive control functions, *INS* in involved in autonomic function, emotion and decision making among several others. *MSMN* and *VSMN* are involved with sensorimotor functions and *SSNR* and *SSNL* (Figure 4.2, fourth row) are involved with various somatosensory processes that are particularly relevant to COVID related symptoms in survivors. *BGN* is another relevant network to our hypothesis that consists of regions from the subcortical system and has direct connections to the olfactory system involved with smell function. *SCRB* and *PCRB* are primarily networks from the cerebellar system.

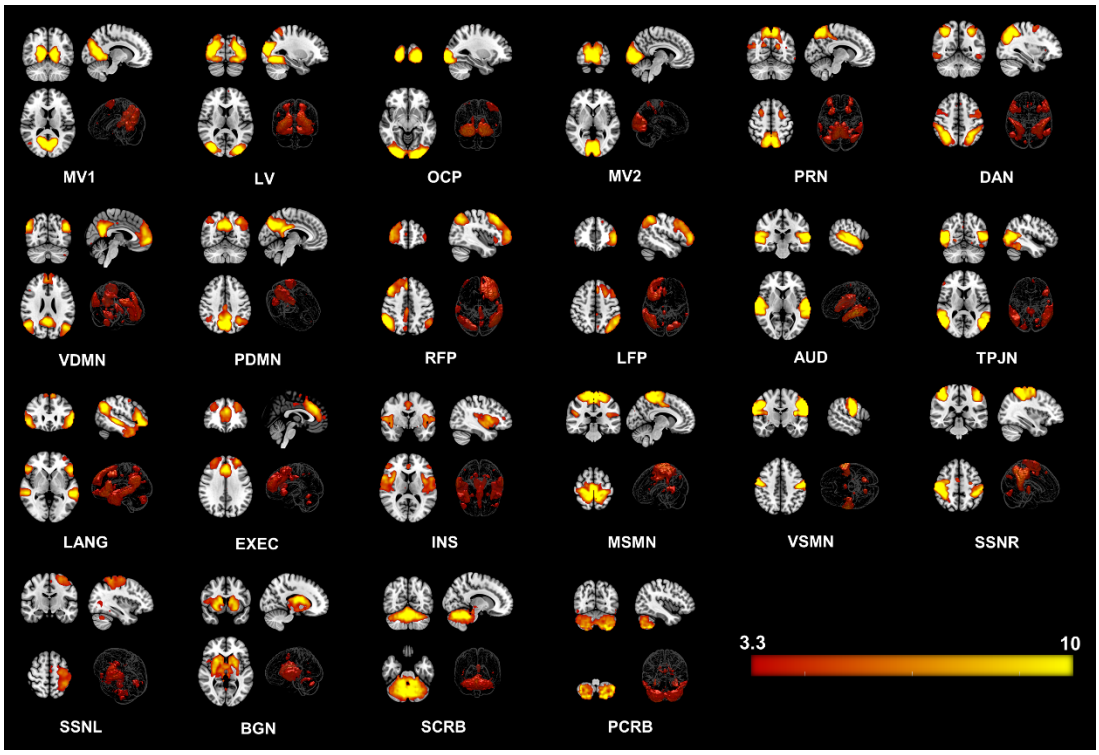

Figure 4.2 Twenty-two Resting State Networks (RSNs) identified from group ICA using 'melodic'. Abbreviated names of each network are shown at the bottom of each image. Three orthogonal slices are shown for each network along with a volume rendered image to show depth and three-dimensional view of the RSNs. Statistical estimates (Z-scores) are embedded into a colorbar at the bottom-right. Keys: MV1 = Medial Visual 1, LV = Lateral Visual, OCP = Occipital Pole, MV2 = Medial Visual 2, PRN = Precuneus Network, DAN = Dorsal Attention, VDMN = Ventral Default Mode Network (DMN), PDMN = Posterior DMN, RFP = Right Fronto Parietal, LFP = Left Fronto Parietal, AUD = Auditory, TPJN = Temporo-Parietal Junction Network, LANG = Language Network, EXEC = Executive Control Network, INS = Insular Network, MSMN = Medial Sensory-Motor Network (SMN), VSMN = Ventral SMN, SSNR = Somatosensory Network - Right, SMNL = Somatosensory Network - Left, , BGN = Basal Ganglia Network, SCRB = Superior Cerebellar Network, PCRB = Posterior Cerebellar Network.

Figure 4.3 shows the results from the group level analysis from three out of four specific RSNs that were statistically tested to identify FC differences across groups. From the top row, Figure 4.3 (A) demonstrates regions with significantly enhanced FC in the HC group when compared to the LOS group for the *BGN* network with *right – gyrus rectus (GRe), medial frontal cortex (MFC)* and *middle orbital gyrus (MOrG)*.

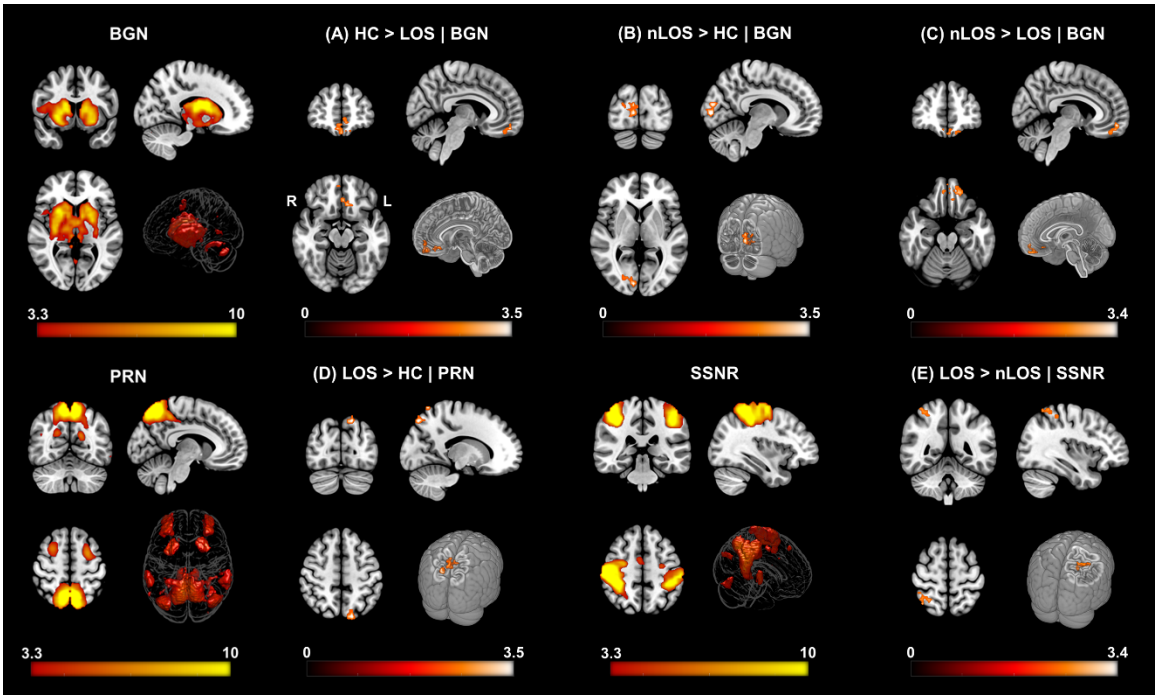

Figure 4.3 ΔFC | Functional Connectivity differences between COVID survivors and healthy controls. [Top row] (A) HC > LOS: Enhanced FC in HC compared to LOS group observed for the *BGN* network (top row, left) with regions from the *medial* and *orbital frontal gyrus*. Three orthogonal slices along with a cut-to-depth volume rendered image show the effects in the cluster comprising of *92 voxels*, with peak *t-score* of $T = 4.01$ and *FWE corrected p-value* of $p_{fwe} = 0.0003$. The colorbar represents t – score values. (B) nLOS > HC: Enhanced FC in nLOS group compared to HCs observed for *BGN* network with regions from the *calcarine cortex.* The cluster size was *71 voxels,* with peak $T = 3.97$ and $p_{fwe} = 0.003$. (C) nLOS > LOS: Enhanced FC in nLOS group compared to LOS observed for *BGN* network with regions from the *medial* and *orbito-frontal gyrus.* The cluster comprised of *66 voxels,* with $T = 3.61$ and $p_{fwe} = 0.005$. [Bottom row] (D) LOS > HC: FC within the *PRC* network (bottom row, left) was enhanced in the LOS group compared to the HC group with regions from the *right superior parietal lobe*. The cluster size was *96 voxels,* with peak $T = 4.05$ and $p_{fwe} = 0.0003$. (E) HC > COVID: Enhanced FC in LOS compared to nLOS observed in the *SSNR* (bottom row, third column) network with regions from the *left superior parietal lobe*. The cluster comprised of *49 voxels,* with peak $T = 3.57$ and $p_{fwe} = 0.038$. Note, the red-yellow colorbar represents Z-scores, representing group level large scale RSN from which the group differences were obtained.

For the *BGN* network, enhanced FC was also observed in nLOS group compared to HC group (Figure 4.3 (B)), with *right – calcarine cortex (Calc), lingual gyrus (LiG)* and *cuneus (Cun)*. Interestingly, FC was also altered within COVID subtypes for the *BGN* network. Figure 4.3 (C) shows that FC was enhanced in the nLOS group when compared to LOS group with *bilateral – medial frontal cortex (MFC), medial segment of the superior*

frontal gyrus (MSFG), middle orbital gyrus (MOrG) and *gyrus rectus (GRe)*. Please note, the first image in the top row of Figure 4.3 represents the large-scale *BGN* network that was obtained from the group ICA. This is provided as a reference to show which network exhibited the FC alterations.

The bottom row of Figure 4.3 shows LOS group had enhanced FC within the *PRC* and *SSNR* networks when compared to HC and nLOS groups, respectively. Particularly, within the *PRC* network (Figure 4.3, bottom row, left), FC was enhanced with *left – superior parietal lobule (SPL), superior occipital gyrus (SOG)* and *precuneus (PCu)*. For the *SSNR* network (Figure 4.3, bottom row, third column), FC was enhanced with the *right – SPL, angular gyrus (AnG)* and *supramarginal gyrus (SMG)*.

The cluster details with relevant anatomical locations based on the standard MNI space have been tabulated in Table 4.1 for reference. Table 4.1 also provides statistical information pertaining to the cluster size, the peak *t-score* and corrected *p-values* after accounting for multiple comparisons. The direction of such changes between groups i.e., if FC is enhanced or reduced compared to the other group is provided in the 'ΔFC' column. More information can be found from the 'Keys' provided at the bottom of the table.

4.4 Discussion

The statistical results from the functional data metrics, particularly, ALFF and FC support our hypothesis that hyposmic and non-hyposmic subtypes among COVID survivors, demonstrate altered local brain activity and FC compared to HCs. Interestingly, brain regions with altered BOLD activity and FC from our analysis match to single case reports with structural and functional alterations, as well as cohort specific group reports from

current literature. In this section, we expand on these findings and compare our results to interpret the results scientifically.

Table 4.1 List of Spatial Regions with Significant FC Differences Across Groups

ΔFC	RSN/ (R/L)	Anatomical Locations	Cl. Size	MNI Co. X	Y	Z	Peak t, p_{fwe}
HC > LOS	*BGN (R)*	*Gyrus Rectus (GRe)*	92	6	51	-18	4.46, 0.004
		Middle Frontal Cortex (MFC)					
		Middle Orbital Gyrus (MOG)					
nLOS > HC	*BGN (R)*	*Calcarine Cortex (Calc)*	71	9	-87	3	3.97, 0.003
		Lingual Gyrus (LiG)					
		Cuneus (Cun)					
nLOS > LOS	*BGN (R-L)*	*Middle Frontal Cortex (MFC)*	66	6	51	-12	3.61, 0.005
		Medial Segment of Superior Frontal Gyrus (MSFG)					
		Middle Orbital Gyrus (MOG)					
		Gyrus Rectus (GRe)					
LOS > HC	*PRN (L)*	*Superior Parietal Lobule (SPL)*	96	-15	-78	51	4.05, 0.0003
		Precuneus (PCu)					
		Superior Occipital Gyrus (SOG)					
LOS > nLOS	*SSNR (R)*	*Superior Parietal Lobule (SPL)*	49	36	-57	60	3.57, 0.038
		Angular Gyrus (AnG)					
		Supramarginal Gyrus (SMG)					

Keys: ΔFC = contrast for difference in functional connectivity between two groups, RSN = resting state networks, (R/L) = right or left hemisphere of the brain, Cl. Size = cluster size in voxels, MNI Co. = Montreal Neurological Institute Coordinates in X, Y and Z planes, Peak *t,* p_{fwe} = peak *t-score* and *fwe* corrected *p value* of the cluster

4.4.1 Higher ALFF in Hyposmic and Non-Hyposmic Survivors

We observed higher local BOLD activity (ALFF) in both nLOS and LOS groups, when compared to HCs. Specifically, for the hyposmic (LOS) group, higher ALFF was observed in the *orbital gyrus* (*POrG, MOrG*), *limbic system* (*Hc, PHG, Amg), basal ganglia* (*Pd, BsF, Pu*) and from *the temporal lobe (Ent, TP)*. Interestingly, the regions from the *orbital gyrus*, *limbic system* and *basal ganglia* have direct neuroanatomical connections to the olfactory cortex (Amunts et al., 2005; Soudry et al., 2011) and association with emotional processing (Damasio & Damasio, 1994). Compared to HC group, we also observed higher ALFF in the nLOS group, specifically in *right basal ganglia (Pu, Cd, BsF, Pd)* and the *limbic system* (*Hc, PHG, Amg*). Particularly for the regions in the *limbic system,* we also observed abnormal GMV in the hyposmic group from our VBM analysis. Moreover, structural alterations in single patient cases with hyperintensities observed from FLAIR imaging match with the spatial locations observed here. Regions from the *basal ganglia*, *limbic system* and *temporal lobe* were reported to be hyperintense from several acute case reports (Kandemirli et al., 2020; Kremer et al., 2020; Paterson et al., 2020).

Exclusively, in patients with olfactory dysfunction several MRI reports depict abnormal intensities (Laurendon et al., 2020; C.-W. Li et al., 2020; Politi et al., 2020) as well as asymmetry in the olfactory system (Coolen et al., 2020). Even with fMRI abnormal BOLD activity has been reported in the piriform cortex from a female patient with abnormal smell function (Ismail & Gad, 2021). More importantly, the regions with higher ALFF from the LOS group match these reports. Therefore, our results from ALFF analysis indicate a link between structural alterations and abnormal local brain activity in regions directly involved with olfactory function.

4.4.2 Altered ICA in Hyposmic and Non-Hyposmic Survivors

Our hypothesis relating to FC analysis was based on both early case-reports and more recent group level neuroimaging reports of structural and functional brain alterations. Individual case reports were primarily from acutely ill patients using FLAIR (Kandemirli et al., 2020; Kremer et al., 2020; Paterson et al., 2020) and Susceptibility Weighted Imaging (SWI) (Conklin et al., 2021), whereas, group level reports, such as those derived from fMRI, include, reduced *default mode* and *salience* connectivity (Fischer et al., 2021) and high prevalence of abnormal time varying and topological organizations between *sensorimotor* and *visual* networks (Fu et al., 2021). In the current context, we report between group FC alterations of three large scale RSNs – *BGN*, *PRN* and *SSNR* networks among COVID subtypes and HCs.

It is important to report group level effects across different sites to evaluate if the single case reports from those sites can be reliably replicated across different countries in specific cohorts. This also demands that the neuroimaging literature now move towards reliable group level estimates, especially those involving fMRI. This allows a more conclusive and clearer picture of the brain changes in a group of patients. For example, while initially a single patient showed no differences in FC of *DMN* when compared to five healthy controls (Fischer et al., 2020), Fischer and colleagues recently reported reduced FC within *DMN* and between *DMN* and *SAL* networks after group level assessment (Fischer et al., 2021). In the current study, we did not observe any significant alterations in *posterior* or *ventral DMN* (*PDMN* and *VDMN*) networks, but our patient group was not unresponsive and as acutely ill as the patients reported in (Fischer et al., 2021). However, we did observe differences in FC for the *PRN* network which consists of *Precuneus (PCu),*

Frontal Eye Fields (FEF) and parts of the *Superior Parietal Lobule (SPL)*. Enhanced FC of this network was observed with the *SPL* and *PCu* regions in the LOS group when compared to HC group. *PCu* is a constituent of DMN, and higher functional connectivity with this region may indicate some compensatory mechanism due to loss in connections in other pathways.

Furthermore, *SPL* is a constituent of the *posterior parietal cortex (PPC)* which has been shown to have functional association with altered *anterior insula* connectivity in chronic fatigue syndrome (CFS) (Wortinger et al., 2017). This is important because fatigue is the most frequently reported symptom among survivors. In Chapter 3, we showed from our participant demographics statistics that fatigue was also the highest reported symptom in our sample (> 86%). We discuss more on this issue separately in the next chapter (see Chapter 5). Moreover, these brain regions are also known to be involved in attention processing, therefore, enhanced FC in these regions may indicate possible compensatory mechanisms of attention related symptoms that recovering patients may experience. Therefore, further investigations are necessary to understand these processes better, especially, from a clinical perspective.

Interestingly, for *BGN*, the LOS group demonstrated reduced FC in regions from the *medial* and *orbito-frontal gyri* (*MOrG, GRe*, *MFC*), when compared to both HC and nLOS groups. These regions are constituent of the olfactory system and *BGN* have direct anatomical connections with this system. This can indicate why the LOS group experience a loss or reduction in smell function. Compared to HC group, enhanced FC in the nLOS group was also observed for the *BGN* network with regions from the occipital lobe (*Calc, Cu* and *LiG*). *Calc* and *Cu* are primarily involved in visual processing. Fu and colleagues

reported that COVID survivors had higher connectivity between *Cerebellum*, *Sensorimotor* and *Visual* networks, indicating they spent abnormally higher time in a specific brain state compared to healthy controls (Fu et al., 2021). A recent study has also suggested *Cu* to be a major hub for mild cognitive impairment in idiopathic REM sleep behavior disorder (iRBD) (Mattioli et al., 2021). *LiG* and weak *insular* coactivation with the *occipital* cortex have been shown to be associated with disrupted salience processing that can lead to loss in motivation in day-to-day tasks (Kim et al., 2018). Moreover, the *basal ganglia* are known to be associated with fatigue (Miller et al., 2014), cognitive, emotional and attention processing (Di Martino et al., 2008; van Schouwenburg et al., 2015).

We also observed significantly reduced FC in the nLOS group compared to LOS group within the *SSNR* network with *right SPL, AnG, SMG* regions. The somatosensory network plays a central role in processing body related stimuli. FC irregularities in the somatosensory cortex have been shown using RS-fMRI in several conditions such as eating disorder or bulimia, depression, and insomnia (Favaro et al., 2012; Kang et al., 2018; Lavagnino et al., 2014; Wang et al., 2018). This could indicate a link between other body related symptoms such as lack of sleep or appetite among non-hyposmic survivors.

4.4.3 Conclusion

The synergy of these studies to our findings indicates possible functional brain associations with commonly observed symptoms in COVID survivors. Particularly, these symptoms last many months (Carfì et al., 2020; Garrigues et al., 2020; Logue et al., 2021; Peluso et al., 2021) in post-acute sequelae SARS-CoV-2 infection (PASC or Long COVID) patients. FC alterations in multiple networks also suggest that RS-fMRI can be useful to investigate multiple brain networks across the whole brain (Damoiseaux et al., 2006; Raichle &

Mintun, 2006; Shulman et al., 2004) in COVID-19 survivors. The results also suggest a possible link between structural and functional abnormalities in COVID survivors. More specifically, for the hyposmic group, the FC alterations associated with olfaction were observed in brain regions that align with anatomical abnormalities.

CHAPTER 5

THE RELATION OF BRAIN ESTIMATES WITH FATIGUE

Chapters 3 and 4 highlighted structural and functional brain abnormalities among COVID survivors. This chapter describes how these brain estimates correlate to self-reported fatigue at work across the groups. First the background in support of the hypothesis being tested is presented. Then, the effects across groups are presented for VBM and FC estimates, respectively, and discussed in terms of fatigue-related literature.

5.1 Introduction

5.1.1 Background

A rising concern with surviving COVID patients have been development of a sequela of symptoms (Logue et al., 2021; Peluso et al., 2021; Tabacof et al., 2020) which converge to the brain as the responsible organ. Therefore, changes in brain structure and function could correlate to the severity of these symptoms. In regard to that, a follow-up study (Tu et al., 2021) assessed structural and functional changes related to post-traumatic stress symptoms (PTSS), where they investigated COVID-19 patients in two consecutive time points - 3 months and 6 months after initial infection. The self-reported Posttraumatic Stress Disorder Checklist for DSM-5 (PCL-5) scores from COVID subjects were negatively correlated to left hippocampal and amygdala volumes. The interval after hospital discharge can also be a modulating factor and therefore, severity of symptoms can be different across time. For example, the study from Tu et al., 2021 also show that the PCL-5 scores from Session 1, i.e., after 3 months, correlated with the time after discharge and the total PCL-5 scores from

these survivors increased by ~20% after 6 months at Session 2 (Tu et al., 2021). Furthermore, another study (Duan et al., 2021) shows that the modified Rankin Scale (mRS), a clinical disability score, significantly correlated with lower GMV in the frontal lobe both during discharge and after a 6 month-follow-up. It is possible that structural changes could be caused by inflammatory storms, which can be identified at the acute stage. For example, a recent study (Qin et al., 2021) reported that the left hippocampal cortical thickness was negatively correlated with the inflammatory biomarker procalcitonin (PCT) in the severe group. Since fatigue is the highest reported symptom from surviving patients (Logue et al., 2021; Peluso et al., 2021; Tabacof et al., 2020), we wanted to ask, if self-reported fatigue (during work) independently correlated to voxel-wise GMV in regions, known to be functionally associated with fatigue. We hypothesized that across groups (HC and COVID), a significant correlation of GMV with self-reported fatigue scores will be observed and the effects of the COVID group (LOS and nLOS) will be stronger compared to the HC group.

It is possible that brain metrics derived from functional data, such as functional connectivity (FC), also demonstrate correlation with fatigue. Since several of the long-COVID symptoms suggest cognitive abnormalities among survivors, most contemporary neuroimaging studies have turned their attention to behavioral correlates of functional brain alterations, primarily, post-traumatic stress syndromes (Benedetti et al., 2021; Fu et al., 2021). On the other hand, several others have attempted to use functional connectivity (FC) as a neurobiological indicator of higher stress levels (Liu et al., 2021; Perica et al., 2021), depression (Zhang et al., 2022) and negative affect (Xiao et al., 2021) among only healthy subjects before and after the pandemic. Therefore, we further hypothesized that across

groups (HC and COVID), a significant correlation between FC and self-reported fatigue scores will be observed and the effects will be larger in the COVID group compared to the HC group.

5.1.2 Statistical Analysis

To evaluate the relationship between GMV and fatigue in the sub-set of COVID and HC participants, we performed a voxelwise multiple linear regression analysis, with GMV as the response variable and the fatigue scores as the covariate of interest, while, age, sex and TIV were included as covariates of no interest. Regions with significant correlation between GMV and fatigue score were identified using non-stationary cluster-based thresholding at height threshold $p_{unc} < 0.01$ and *FWE* corrected at $p_{FWE} < 0.05$, for multiple comparisons.

To visualize the significant linear relationship between the GMV and Fatigue, the average GMV within the significant cluster was obtained from each subject across both groups. These average GMV values were then linearly regressed against the fatigue scores and age, sex and TIV of each participant were regressed out during this step. The mean GMV across the participants were then added back to the residuals and the correlation with fatigue scores was computed and visualized within a scatter plot and a line of best fit with 95% confidence interval. The correlation analysis and the graphical plotting was done using 'inhouse' scripts prepared in RStudio (RStudio, 2021). Please note, since within the COVID group (LOS and nLOS) there was no significant differences in the level of fatigue experienced ($p > 0.05$), the effects of GMV and fatigue was not evaluated in these subtypes separately. Rather the two groups were considered as a COVID group in general and their effects were compared against HC group. Please note, the same statistical methods were

also applied to resting state networks derived from ICA and dual regression analyses applied on RS-fMRI data. For the regression analysis, only age and sex were added as covariates of interest, since TIV is more related to VBM specifically.

5.2 Results

5.2.1 GMV-Fatigue Relationship

The multiple linear regression analysis to compute correlation between self-reported fatigue scores and GMV revealed that the subset of participants ($n_{COVID} = 33$, $n_{HC} = 18$) demonstrated significantly positive correlation with GMV in *Posterior Cingulate Cortex (PCC)*, *Precuneus (PRC)* and *Superior Parietal Lobule (SPL)*, particularly. The top left image in Figure 5.1 shows the significant cluster that comprised of these regions (see Figure 5.1 bottom row, for a multi-slice view). The scatter plot (Figure 5.1, top right) demonstrates the linear relationship *(Spearman's $\rho = 0.34$, $p = 0.016$)* across the whole group between fatigue scores and the GMV of each subject within the cluster. The scatter plot combines data from both groups, and it can be noted that the light pink dots (COVID subjects) have a significantly higher effect compared to the cyan dots (HC subjects). Therefore, while GMV is positively correlated with fatigue across both groups, the overall trend is primarily driven by the effects from the COVID group.

We also observed another cluster, which did not survive the stringent non-stationary clustering threshold (< 3547 voxels), however, the cluster-based thresholding can be somewhat tricky. Often, a larger cluster size may be required for an effect and a true effect may be ignored simply because a *p* value threshold is not reached. It is further limited by sample size and other regressors that lowers the degrees of freedom. We had a

comparatively smaller sample size for the correlation analysis. Therefore, we still wanted to evaluate the effects after extracting the average cluster GMV and performing the linear regression.

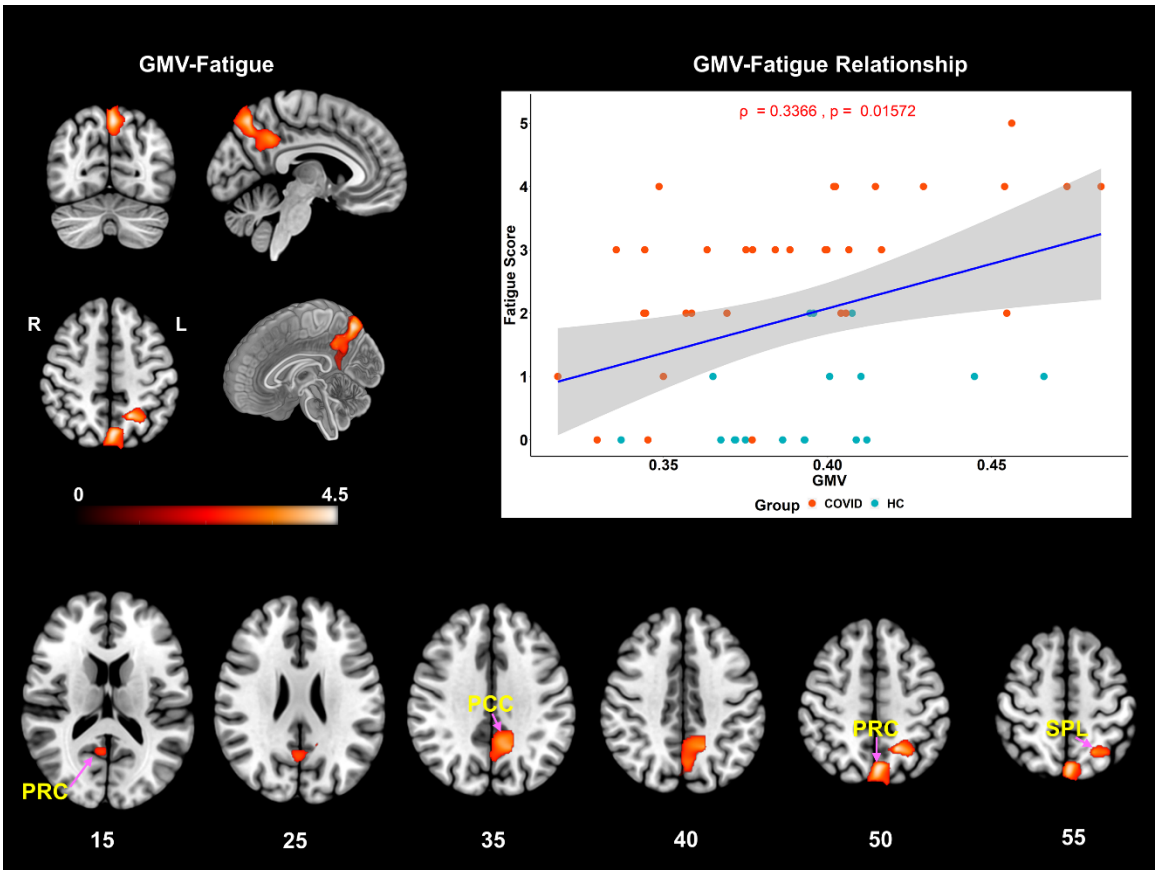

Figure 5.1. VBM demonstrating significantly positive correlation with fatigue scores across the whole group. The significant cluster (top-left) consisting of 3547 voxels (k_E = *3547*), comprised of: *Left – PCC*, PRC, SPL and *Right - PRC* with peak t-score of *4.74* and exact corrected p-value of p_{FWE} = 0.019 at MNI coordinates: *[-16 -54 48]*. The axial slices (bottom) show the spatial extent of the same cluster over finer slices. The scatter plot (top-right) with the linear regression line shows significant positive correlation of GMV with self-reported fatigue score across the whole group *(ρ = 0.34, p = 0.016, r^2 = 0.11)*. Please note, the ρ represents Spearman's rank-order correlation coefficient. The light pink colored dots represent the COVID subjects, and the cyan dots represent the HCs. The COVID group clearly demonstrates higher effects than the HC group. Please note, the GMV in the x-axis represents the residuals plus the mean GMV of the cluster across subjects added back after linear regression. Keys: *PCC = Posterior Cingulate Cortex, PRC = Precuneus, SPL = Superior Parietal Lobule.* The linear plot (blue) represents the least squares regression line (best fit), and the shaded gray area represents the 95% confidence interval.

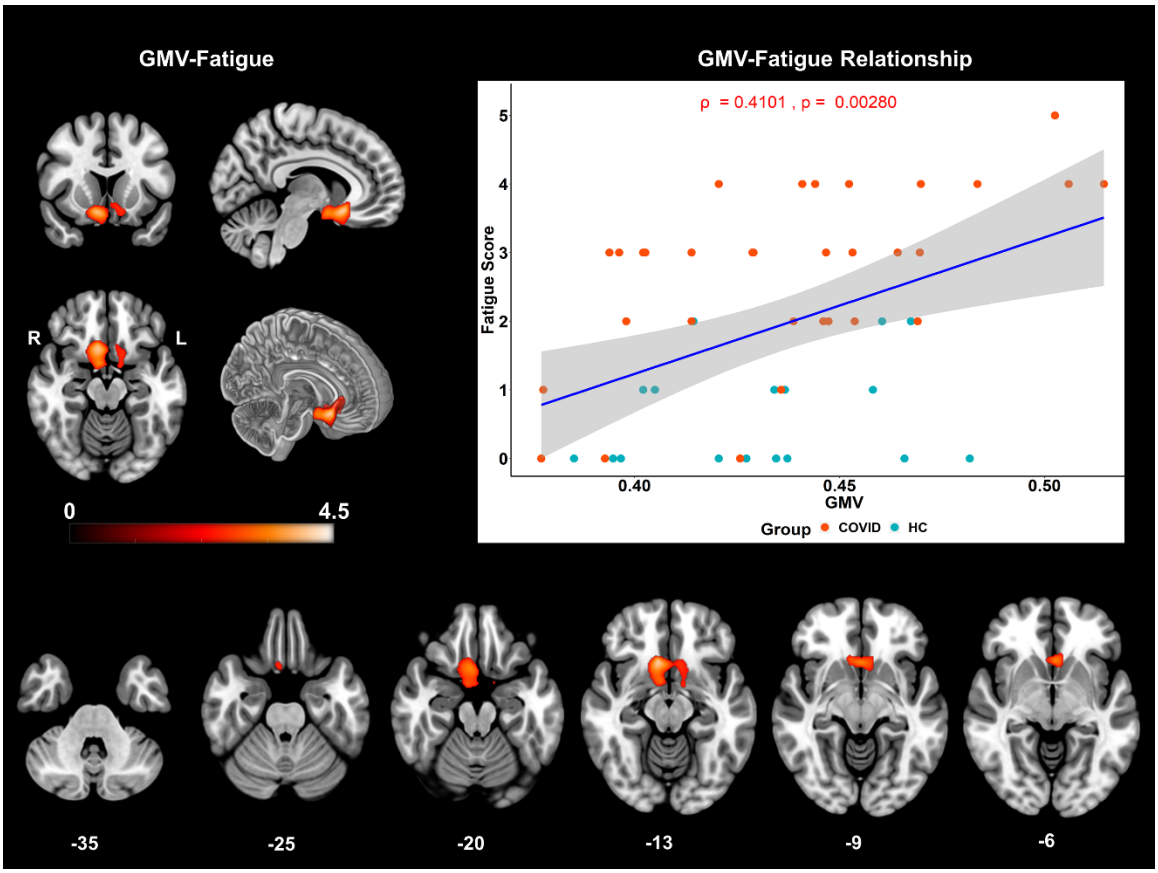

Figure 5.2. VBM demonstrating positive correlation with fatigue scores across the whole group. The cluster (top-left) (1796 voxels) did not survive the non-stationary cluster threshold (k_E = 3547 voxels). However, when the residual plus mean GMV across group was regressed against fatigue scores, a significant effect was observed (top-right). The cluster comprises of *bilateral – Subcallosal Area (ScA), Accumbens Area (AcA), Mid-orbital Gyrus (MOG), Anterior Cingulate Gyrus (ACG), Medial Frontal Cortex (MFC), Gyrus Rectus (GRe), Caudate (Cd), Putamen (Pu) and Bilateral – Ventral Diencephalon (VDC) and Right – Basal Forebrain (BsF), Amygdala (Amg), Entorhinal Area (EnA) and Parahippocampal Gyrus (PHG)*. A multi-slice axial view has also been added to showcase the spatial extent of this cluster. The linear plot (blue) represents the least squares regression line (best fit), and the shaded gray area represents the 95% confidence interval.

When the residual plus average cluster GMV was linearly regressed against fatigue, a significant positive correlation (*Spearman's $\rho = 0.41$, $p = 0.0028$*) was observed. This cluster consisted of brain regions from the *cholinergic output* from the *ventral basal ganglia (BsF, AcA), orbitofrontal cortex (MOG, GrE)* and *ventromedial prefrontal cortex (vmPFC) (ACG, MFC)*. Like Figure 5.1, the statistical map, multi-slice view and the linear plot for this cluster are shown in Figure 5.2.

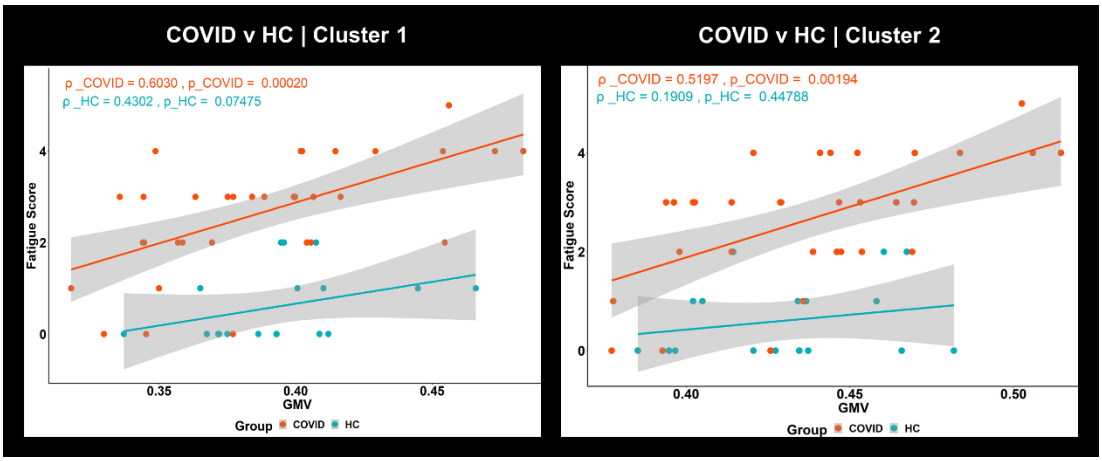

Figure 5.3. Demonstrating GMV-fatigue correlation observed in COVID and HC groups separately. *Left:* Scatter plot and linear regression line for each group from the significant cluster shown in Figure 5.1. *Right:* Similarly stronger effects were also observed for the cluster shown in Figure 5.2. The scatter plots are exactly same as those shown in Figures 5.1 and 5.2, except the regression lines in the current figure shows the effects in each group separately. The plots clearly show that the overall group effects in Figures 5.1 and 5.2 are primarily driven by the COVID group, as GMV in this group is more strongly correlated to fatigue.

To show that the COVID group demonstrated stronger correlation effects compared to the HC group, we also computed the correlations and generated corresponding linear regression plots for each group separately. The plots generated from the first (Figure 5.3, *left*) and second (Figure 5.3, *right*) clusters shown in Figures 5.1 and 5.2 respectively. The scatter plot and the linear regression lines from each group from the significant cluster (Cluster 1, Figure 5.3, *left*) shows more intuitively that the COVID group ($\rho\_COVID = 0.60, p\_COVID = 0.0002$) was more susceptible to fatigue compared to the HC group ($\rho\_HC = 0.43, p\_HC = 0.07$). Similar effects could also be observed for the second cluster (Cluster 2, Figure 5.3, *right*). Interestingly, we can observe that although Cluster 2 did not survive the conservative non-stationary cluster extent threshold for multiple comparisons, there are effects like those observed for Cluster 1. The COVID group showed significantly stronger positive correlation ($\rho\_COVID = 0.52, p\_COVID = 0.002$) compared to HC group ($\rho\_HC = 0.19, p\_HC = 0.45$).

5.2.2 FC-Fatigue Relationship

Figure 5.4 shows brain regions where a significant negative correlation was observed between FC and self-reported fatigue, from the *precuneus* (*PRN)* network. The statistic map (Figure 5.4, *left*) shows the cluster where a negative correlation between FC and fatigue scores was observed in the *Left – Superior Parietal Lobule (SPL), Superior Occipital Gyrus (SOG), Angular Gyrus (AnG)* and *Precuneus (PCu)*. The graph on the right visually presents this negative relationship (*Spearman's* $\rho = -0.47$, $p = 0.001$, $r^2 = 0.22$) between the average FC of this cluster and fatigue scores. The scatter plot (Figure 5.4, *right*) clearly shows that the effects of FC and fatigue are significantly larger in the COVID group (light pink dots higher than cyan dots) compared to HC group.

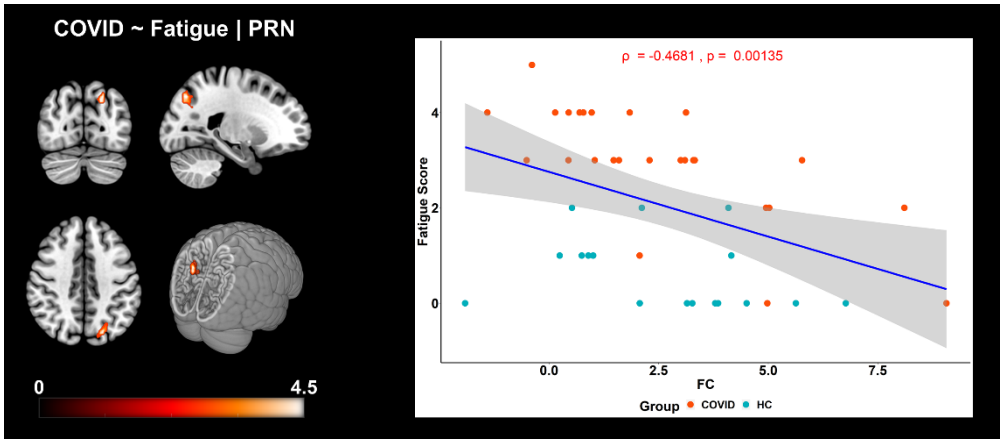

Figure 5.4 Negative correlation of FC with self-reported fatigue scores in COVID and HC individuals. *Left:* For the *PRN* network, three orthogonal slices (left) along with a cut-to-depth volume rendered image showing regions from the *Superior Parietal* and *Occipital* Gyri that demonstrated significantly negative correlation with fatigue. The colorbar represents t-score values. *Right*: The graph shows the linear relationship between FC within the significant cluster and self-reported fatigue scores across all groups. The x-axis represents the residuals plus the average FC (z-scores) across groups from the cluster and the y-axis represents the fatigue scores. The light pink dots represent the COVID group and the cyan dots represent the HC group. The shaded gray area represents the 95% confidence interval. The blue line represents the least squares regression line of best fit. Cluster information include - cluster peak: *[-21 -72 42],* | cluster extent threshold, $k_E = 46$ and cluster size = *46 voxels*. The peak t-score of the cluster was, $T_{peak} = 4.39$, and corrected for multiple comparisons at $p < 0.05$.

5.3 Discussion

5.3.1 Stronger GMV-Fatigue Effects in COVID Survivors

The results from the correlation analysis between GMV and fatigue support the hypothesis that fatigue levels experienced by the COVID survivors will be higher compared to the HC group and GMV will correlate more strongly with self-reported fatigue in this group. Reports have emerged of recovering patients experiencing a sequelae of symptoms that persist from 3-6 months and beyond after initial infection (Logue et al., 2021; Peluso et al., 2021; Tabacof et al., 2020). Fatigue was the highest reported symptom in these studies among others, including lack of attention, delayed recovery of loss of sense of smell and taste. We asked the healthy subjects and surviving patients, what level of fatigue do they experience in their daily work? Based on their reported score, we observed significantly higher levels of fatigue within the COVID group when compared to HCs (see Table 3.2). We also observe from Figure 5.1 that GMV in *PCC, PRC* and *SPL* regions are more strongly correlated to fatigue in COVID survivors compared to healthy controls. This could also indicate a link to high percentage of survivors experiencing fatigue during and post recovery, eventually leading to functional or cognitive disruption. This is also typical of neurodegenerative populations and these regions have been found to be related to fatigue. For example, higher metabolic activity within *PCC* has been shown to be positively correlated with higher fatigue levels in Parkinson's patients (Cho et al., 2017). *PCC* and *SPL* have also been shown to be associated with fatigue in patients with chronic fatigue syndrome (CFS) (Boissoneault et al., 2018; Gay et al., 2016). Moreover, atrophy in the *parietal* lobe has been shown to be associated with fatigue among multiple sclerosis (MS) patients (Calabrese et al., 2010; Pellicano et al., 2010).

We also observed similar effects in another cluster (did not survive non-stationary thresholding, see Figure 5.2) particularly comprising of brain regions from the *ventral basal ganglia (BG)* and *ventromedial prefrontal cortex (vmPFC)*. Interestingly, the *BG* and *vmPFC* regions have also been shown to be functionally associated with fatigue (Chaudhuri & Behan, 2000; Dobryakova et al., 2020; Dobryakova et al., 2015; Dobryakova et al., 2018; Wylie et al., 2017; Wylie et al., 2019). We observed this effect with 18 HCs and 33 COVID subjects and our expectation is that with a bigger sample size in both groups, this cluster would survive and therefore it may be of relevance to fatigue related effects among survivors.

5.3.2 Stronger FC-Fatigue Effects in COVID Survivors

We further evaluated linear relationship between FC of RSNs and self-reported fatigue at work. We observed that the COVID group was significantly more negatively correlated to FC within the *PRC* network compared to the HC group. More specifically, the correlation between FC and fatigue was observed within the *SPL, SOG, AnG* and *PCu,* i.e., brain regions primarily belonging to the *parietal* lobe. Structural atrophy in the *parietal* lobe has been shown to be associated with fatigue among multiple sclerosis (MS) patients (Calabrese et al., 2010; Pellicano et al., 2010). An RS-fMRI study of patients with chronic fatigue syndrome (CFS) used ICA to reveal loss of intrinsic connectivity in the *parietal* lobe (Gay et al., 2016). It is interesting that lower FC of the *PRC* network with regions from the *parietal* lobe correlates negatively to higher fatigue scores among COVID survivors. To the best of our knowledge, this is the first study to show work-related fatigue correlates of FC among recovering patients 2 weeks after hospital discharge. Therefore, future studies are necessary to evaluate this avenue further in the surviving cohorts.

5.3.3 Conclusion

In conclusion, we observed COVID survivors experience higher levels of fatigue compared to HCs. We noticed that fatigue is significantly correlated with GMV and FC and these effects are more strongly observed in the hyposmic and non-hyposmic survivors compared to HCs. More importantly, these effects have functional implications, because the brain regions demonstrating these stronger effects with fatigue are also known to be functionally associated with fatigue from other studies.

CHAPTER 6

CHALLENGES, LIMITATIONS AND FUTURE DIRECTIONS

Chapters 3, 4 and 5 depict the methods applied for all three aims of this study and the results that provide evidence in support of our hypotheses that were tested. Neuroimaging studies have their own caveats in terms of spatial and temporal resolution. For both structural and functional modalities, there are challenges faced ubiquitously among research groups. Aside from such standard limitations, each study comes with its own challenges and our study is no different in that aspect. Here we discuss some limitations and challenges from the initiation of the study to its current stage. We also suggest possible adaptations that may be implemented in overcoming some of these limitations in the future.

This study involves COVID patients. Due to the pandemic recruiting healthy controls proved even more difficult. Understandably, the control subjects were in a lot of stress and fear of being exposed to COVID-19 during the early phase of recruitment. This is equally challenging for the COVID survivors who were also afraid of the risk of getting exposed to the virus again. While mask mandates have eased up now, it was not the case when we started scanning the subjects. Extreme precautions were taken during the 1st phase of recruitment just to make sure the patient is not compromised again and does not infect others in the process. Of course, both the healthy and COVID groups had to wear masks through the full process of screening, answering questionnaire and scanning.

A big part of the process was to ensure and convince the participants of their safety in an MRI environment. Not all participants were keen on going under an MRI. We observed a general fear among subjects when discussing an MRI scan. Educating the

participants of the safety protocols and finally getting their consent to come in for a scan is an extremely time consuming and laborious process. This requires additional 'man-power' which becomes almost impossible during a lock down. This is an ongoing study, and we are very interested in the longitudinal progression of the symptoms in these survivors. However, follow-up studies can be challenging for the time required and the perceived risks of subjects going to the hospital and being MRI scanned.

To make sure we have a large enough sample pool to recruit COVID subjects, we contacted the Metro Heart and Super Specialty Hospital, New Delhi, India during the early phase of COVID-19. We were able to recruit 47 COVID subjects from a sample of over 2000 patient database. This abundant flexibility greatly helped in the continuation of the study. It is understandable that 47 subjects may seem insufficient for robust statistical power, but our sample size is quite comparable among current publications with cross-sectional designs (Duan et al., 2021; Fu et al., 2021). We hope that the aforementioned points help explaining why recruiting even these many subjects can be quite difficult under the circumstances.

6.1 Limitations of The Structural Analysis

In the beginning of this study, there were hardly any conclusive group level effects in any specific COVID cohort in the literature. Naturally, we tried to address that by investigating any group level differences between survivors and controls (Hafiz, Gandhi, Mishra, Prasad, Mahajan, Di, et al., 2022). With the availability of more data and participant information, we were able to move to more definite group level hypotheses for the structural analysis in this study. Despite our emphasis on group level analysis, we understand that in a clinical

setting, it may have little transferability, owing to idiosyncrasies associated with each patient. A possible approach to address this issue would be to compare patient specific VBM against a sufficiently sized control sub-group randomly selected from a larger cohort (Scarpazza et al., 2016). However, it may not be very practical in a clinical setting unless a well-designed control dataset is available for a clinician. Nevertheless, our group level results from a single site seem to match single patient findings quite well, especially when they were reported from several centers across different countries (Gulko et al., 2020). Moreover, currently, we only have 47 COVID subjects. While we do observe significant effects across groups, the LOS group had only 17 subjects. We would still need a larger sample size to verify the main effects across these groups more conclusively. The IIT team from India have been collecting new data and about 48% of the newly recruited sample had experienced loss of sense of smell or some form of hyposmia. This opens an opportunity to study the LOS group with larger sample size in the future.

Another concern we had is the reversibility or transient nature of some effects. These patients were scanned two weeks after hospital discharge. It is possible some critical effects may have already disappeared through recovery or reversible neurological processes. But it was also necessary to allow for that 2-week interval to remove any hospitalization factors confounding COVID-related effects in the brain. Therefore, a better approach could be to scan the patients at onset, during and after recovery along with behavioral parameters to assess any possible trends unique to the neurological pathology in COVID survivors. That is indeed, where this study is heading with the hope that more participants agree to come back for the second and third scan after 6 and 12 months respectively.

6.2 Limitations of The Functional Analysis

If we look at the early neuroimaging literature, the first functional imaging studies were also case reports (Fischer et al., 2020; Ismail & Gad, 2021). Therefore, the need to move from single cases to group level effects was equally, if not more, relevant for the functional neuro-imaging field. Despite our efforts to show group level effects that reflect individual and group level reports in the recent literature (Hafiz, Gandhi, Mishra, Prasad, Mahajan, Natelson, et al., 2022), our study still maintains a cross-sectional design. In cases like this, a better approach for the future would be to use follow up designs (Fu et al., 2021; Lu et al., 2020; Tu et al., 2021) or possibly a longitudinal design where patients could be observed both before and after the pandemic like the one using the UK-biobank (Douaud et al., 2021). Our effort here, was to delineate the functional differences between hyposmic, non-hyposmic and healthy subjects at an early stage of recovery (2 weeks after hospital discharge) and determine the relation between work-related fatigue and FC of RSNs. We believe the results from this study will help understanding the recovery stage brain alterations and how they might drive fatigue-related symptoms among COVID survivors.

In the future, with more data collection, follow-up and longitudinal assessments can be made. The parameters obtained from the first time point can be used to assess if they can predict development of brain pathologies among these subtypes. One expectation is that these early differences in the hyposmic group and the higher susceptibility to fatigue among the COVID participants, will be an early indicator to PASC development and other fatigue related disturbances such as chronic fatigue syndrome (CFS) in these survivors. Dr. Benjamin H. Natelson, from the Neurology department in Mount Sinai, is an expert in CFS. Based on his expert evaluation, the symptoms of fatigue observed in the COVID survivors

closely resemble those of CFS. He thinks identifying these abnormalities at an earlier point in recovery which may contribute to PASC and CFS development are paramount. Therefore, this could be clinically relevant and potentially help come up with better strategies against such brain pathologies early in the recovery phase.

6.3 Limitations of The Fatigue Correlation Analysis

We evaluated brain correlates of fatigue and compared the regression models of COVID and HC participants based on self-reported scores during work. The questionnaire was set on a scale of 0-5, with increasing fatigue levels towards 5. While these scores helped us identify fatigue related effects in the brain in these survivors, perhaps a more clinically relevant test is preferred. Unfortunately, there is no single test to evaluate a complex symptom like fatigue or CFS. Nevertheless, the fatigue-expert in our study, Dr. Benjamin H. Natelson, believes these scores still prove useful from a research standpoint.

The other challenge in this analysis is the sample size. We were able to obtain scores from 33/47 COVID and 18/35 HC participants. This largely affects the degrees of freedom for statistical tests and reduce statistical power of the effects of interest. However, we were still able to extract significant effects with this sample. Naturally, these effects will need to be verified with a larger sample for a more conclusive inference.

6.4 Conclusion

In this study, we were able to identify structural and functional differences between COVID survivors and HCs. We were further able to differentiate brain abnormalities between two important sub-types among COVID survivors: hyposmic and non-hyposmic

patients. We found that COVID survivors are more strongly affected by fatigue compared to HCs. We find these results interesting because they can have clinical implications towards PASC development among long-haul survivors. We hope these findings will inspire researchers to ask more pertinent questions and help closing the gaps in knowledge using state-of-the-art imaging modalities. We speculate that single imaging modalities will not be sufficient and suggest that a multi-modal approach will provide more conclusive evidence to solve the mysteries behind CNS invasion of the novel coronavirus.

REFERENCES

(WHO), W. H. O. (2022). *WHO Coronavirus (COVID-19) Dashboard*. World Health Organization Coronavirus (COVID-19) Dashboard. Retrieved 02/12/2022 from https://covid19.who.int/table

Abell, F., Krams, M., Ashburner, J., Passingham, R., Friston, K., Frackowiak, R., Happé, F., Frith, C., & Frith, U. (1999). The neuroanatomy of autism: a voxel-based whole brain analysis of structural scans. *Neuroreport*. 1999 Jun 3;10(8):1647-51. doi: 10.1097/00001756-199906030-00005. PMID: 10501551.

Allen, M., Poggiali, D., Whitaker, K., Marshall, T. R., Van Langen, J., & Kievit, R. A. (2021). Raincloud plots: a multi-platform tool for robust data visualization. *Wellcome Open Research*, *4*, 63. https://doi.org/10.12688/wellcomeopenres.15191.2

Altmann, A., Ng, B., Landau, S. M., Jagust, W. J., & Greicius, M. D. (2015). Regional brain hypometabolism is unrelated to regional amyloid plaque burden. *Brain*, *138*(Pt 12), 3734-3746. https://doi.org/10.1093/brain/awv278

Amunts, K., Kedo, O., Kindler, M., Pieperhoff, P., Mohlberg, H., Shah, N. J., Habel, U., Schneider, F., & Zilles, K. (2005). Cytoarchitectonic mapping of the human amygdala, hippocampal region and entorhinal cortex: intersubject variability and probability maps. *Anatomy and Embryology*, *210*(5), 343-352. https://doi.org/10.1007/s00429-005-0025-5

Ashburner, J. (2007). A fast diffeomorphic image registration algorithm. *Neuroimage*, *38*(1), 95-113. https://doi.org/10.1016/j.neuroimage.2007.07.007

Ashburner, J., & Friston, K. J. (2000). Voxel-Based Morphometry—The Methods. *Neuroimage*, *11*(6), 805-821. https://doi.org/https://doi.org/10.1006/nimg.2000.0582

Ashburner, J., & Friston, K. J. (2009). Computing average shaped tissue probability templates. *Neuroimage*, *45*(2), 333-341. https://doi.org/10.1016/j.neuroimage.2008.12.008

Behzadi, Y., Restom, K., Liau, J., & Liu, T. T. (2007). A component based noise correction method (CompCor) for BOLD and perfusion based fMRI. *Neuroimage*, *37*(1), 90-101. https://doi.org/10.1016/j.neuroimage.2007.04.042

Biswal, B., Yetkin, F. Z., Haughton, V. M., & Hyde, J. S. (1995). Functional connectivity in the motor cortex of resting human brain using echo-planar MRI. *Magn Reson Med*, *34*(4), 537-541.

Benedetti, F., Palladini, M., Paolini, M., Melloni, E., Vai, B., De Lorenzo, R., Furlan, R., Rovere-Querini, P., Falini, A., & Mazza, M. G. (2021). Brain correlates of depression, post-traumatic distress, and inflammatory biomarkers in COVID-19 survivors: A multimodal magnetic resonance imaging study. *Brain, Behavior, & Immunity - Health*, *18*, 100387-100387. https://doi.org/10.1016/j.bbih.2021.100387

Biswal, B. B., Mennes, M., Zuo, X.-N., Gohel, S., Kelly, C., Smith, S. M., Beckmann, C. F., Adelstein, J. S., Buckner, R. L., Colcombe, S., Dogonowski, A.-M., Ernst, M., Fair, D., Hampson, M., Hoptman, M. J., Hyde, J. S., Kiviniemi, V. J., Kötter, R., Li, S.-J., . . . Milham, M. P. (2010). Toward discovery science of human brain function. *Proceedings of the National Academy of Sciences*, *107*(10), 4734-4739. https://doi.org/10.1073/pnas.0911855107

Boissoneault, J., Letzen, J., Lai, S., Robinson, M. E., & Staud, R. (2018). Static and dynamic functional connectivity in patients with chronic fatigue syndrome: use of arterial spin labelling fMRI. *Clinical Physiology and Functional Imaging*, *38*(1), 128-137. https://doi.org/10.1111/cpf.12393

Bornhövd, K., Quante, M., Glauche, V., Bromm, B., Weiller, C., & Büchel, C. (2002). Painful stimuli evoke different stimulus-response functions in the amygdala, prefrontal, insula and somatosensory cortex: a single-trial fMRI study. *Brain*, *125*(Pt 6), 1326-1336. https://doi.org/10.1093/brain/awf137

Beckmann, C. F., Mackay, C. E., Filippini, N., and Smith, S. M. (2009). Group comparison of resting-state FMRI data using multi-subject ICA and dual regression. *Organization of Human Brain Mapping*.

Calabrese, M., Rinaldi, F., Grossi, P., Mattisi, I., Bernardi, V., Favaretto, A., Perini, P., & Gallo, P. (2010). Basal ganglia and frontal/parietal cortical atrophy is associated with fatigue in relapsing-remitting multiple sclerosis. *Mult Scler*, *16*(10), 1220-1228. https://doi.org/10.1177/1352458510376405

Carfì, A., Bernabei, R., Landi, F., & Gemelli Against, C.-P.-A. C. S. G. (2020). Persistent Symptoms in Patients After Acute COVID-19. *The Journal of the American Medical Association*, *324*(6), 603-605. https://doi.org/10.1001/jama.2020.12603

Chaudhuri, A., & Behan, P. O. (2000). Fatigue and basal ganglia. *J Neurol Sci*, *179*(S 1-2), 34-42. https://doi.org/10.1016/s0022-510x(00)00411-1

Cho, S. S., Aminian, K., Li, C., Lang, A. E., Houle, S., & Strafella, A. P. (2017). Fatigue in Parkinson's disease: The contribution of cerebral metabolic changes. *Hum Brain Mapp*, *38*(1), 283-292. https://doi.org/10.1002/hbm.23360

Cole, D. M., Smith, S. M., & Beckmann, C. F. (2010). Advances and pitfalls in the analysis and interpretation of resting-state FMRI data. *Front Syst Neurosci*, *4*, 8. https://doi.org/10.3389/fnsys.2010.00008

Conklin, J., Frosch, M. P., Mukerji, S. S., Rapalino, O., Maher, M. D., Schaefer, P. W., Lev, M. H., Gonzalez, R. G., Das, S., Champion, S. N., Magdamo, C., Sen, P., Harrold, G. K., Alabsi, H., Normandin, E., Shaw, B., Lemieux, J. E., Sabeti, P. C., Branda, J. A., . . . Edlow, B. L. (2021). Susceptibility-weighted imaging reveals cerebral microvascular injury in severe COVID-19. *Journal of the Neurological Sciences*, *421*, 117308-117308. https://doi.org/10.1016/j.jns.2021.117308

Coolen, T., Lolli, V., Sadeghi, N., Rovai, A., Trotta, N., Taccone, F. S., Creteur, J., Henrard, S., Goffard, J. C., Dewitte, O., Naeije, G., Goldman, S., & De Tiège, X. (2020). Early postmortem brain MRI findings in COVID-19 non-survivors. *Neurology*, *95*(14), e2016-e2027. https://doi.org/10.1212/wnl.0000000000010116

Cox, R. W. (1996). AFNI: software for analysis and visualization of functional magnetic resonance neuroimages. *Comput Biomed Res*, *29*(3), 162-173.

Damasio, A. R., & Damasio, H. (1994). Cortical systems for retrieval of concrete knowledge: The convergence zone framework. In *Large-scale neuronal theories of the brain.* Cambridge, Massachusetts: The MIT Press; pp. 61-74.

Damoiseaux, J. S., Rombouts, S. A., Barkhof, F., Scheltens, P., Stam, C. J., Smith, S. M., & Beckmann, C. F. (2006). Consistent resting-state networks across healthy subjects. *Proc Natl Acad Sci U S A*, *103*(37), 13848-13853. https://doi.org/10.1073/pnas.0601417103

De Luca, M., Beckmann, C. F., De Stefano, N., Matthews, P. M., & Smith, S. M. (2006). fMRI resting state networks define distinct modes of long-distance interactions in the human brain. *Neuroimage*, *29*(4), 1359-1367. https://doi.org/10.1016/j.neuroimage.2005.08.035

del Rio, C., Collins, L. F., & Malani, P. (2020). Long-term Health Consequences of COVID-19. *The Journal of the American Medical Association*, *324*(17), 1723-1724. https://doi.org/10.1001/jama.2020.19719

Di Martino, A., Scheres, A., Margulies, D. S., Kelly, A. M., Uddin, L. Q., Shehzad, Z., Biswal, B., Walters, J. R., Castellanos, F. X., & Milham, M. P. (2008). Functional connectivity of human striatum: a resting state FMRI study. *Cereb Cortex*, *18*(12), 2735-2747. https://doi.org/10.1093/cercor/bhn041

Dobryakova, E., Genova, H., Schneider, V., Chiaravalloti, N. D., Spirou, A., Wylie, G. R., & DeLuca, J. (2020). Reward presentation reduces on-task fatigue in traumatic brain injury. *Cortex*, *126*, 16-25. https://doi.org/10.1016/j.cortex.2020.01.003

Dobryakova, E., Genova, H. M., DeLuca, J., & Wylie, G. R. (2015). The Dopamine Imbalance Hypothesis of Fatigue in Multiple Sclerosis and Other Neurological Disorders [Review]. *Frontiers in Neurology*, *6*(52). https://doi.org/10.3389/fneur.2015.00052

Dobryakova, E., Hulst, H. E., Spirou, A., Chiaravalloti, N. D., Genova, H. M., Wylie, G. R., & DeLuca, J. (2018). Fronto-striatal network activation leads to less fatigue in multiple sclerosis. *Mult Scler*, *24*(9), 1174-1182. https://doi.org/10.1177/1352458517717087

Douaud, G., Lee, S., Alfaro-Almagro, F., Arthofer, C., Wang, C., Lange, F., Andersson, J. L. R., Griffanti, L., Duff, E., Jbabdi, S., Taschler, B., Winkler, A., Nichols, T. E., Collins, R., Matthews, P. M., Allen, N., Miller, K. L., & Smith, S. M. (2021). Brain imaging before and after COVID-19 in UK Biobank. *medRxiv*. https://doi.org/10.1101/2021.06.11.21258690

Duan, K., Premi, E., Pilotto, A., Cristillo, V., Benussi, A., Libri, I., Giunta, M., Bockholt, H. J., Liu, J., Campora, R., Pezzini, A., Gasparotti, R., Magoni, M., Padovani, A., & Calhoun, V. D. (2021). Alterations of frontal-temporal gray matter volume associate with clinical measures of older adults with COVID-19. *Neurobiol Stress*, *14*, 100326. https://doi.org/10.1016/j.ynstr.2021.100326

Dubé, M., Le Coupanec, A., Wong, A. H. M., Rini, J. M., Desforges, M., & Talbot, P. J. (2018). Axonal Transport Enables Neuron-to-Neuron Propagation of Human Coronavirus OC43. *J Virol*, *92*(17). https://doi.org/10.1128/jvi.00404-18

Esposito, F., Cirillo, M., De Micco, R., Caiazzo, G., Siciliano, M., Russo, A. G., Monari, C., Coppola, N., Tedeschi, G., & Tessitore, A. (2022). Olfactory loss and brain connectivity after COVID-19 [https://doi.org/10.1002/hbm.25741]. *Hum Brain Mapp*, https://doi.org/https://doi.org/10.1002/hbm.25741

Fadakar, N., Ghaemmaghami, S., Masoompour, S. M., Shirazi Yeganeh, B., Akbari, A., Hooshmandi, S., & Ostovan, V. R. (2020). A First Case of Acute Cerebellitis Associated with Coronavirus Disease (COVID-19): a Case Report and Literature Review. *Cerebellum (London, England)*, *19*(6), 911-914. https://doi.org/10.1007/s12311-020-01177-9

Favaro, A., Santonastaso, P., Manara, R., Bosello, R., Bommarito, G., Tenconi, E., & Di Salle, F. (2012). Disruption of visuospatial and somatosensory functional connectivity in anorexia nervosa. *Biol Psychiatry*, *72*(10), 864-870. https://doi.org/10.1016/j.biopsych.2012.04.025

Filippini, N., MacIntosh, B. J., Hough, M. G., Goodwin, G. M., Frisoni, G. B., Smith, S. M., Matthews, P. M., Beckmann, C. F., & Mackay, C. E. (2009). Distinct patterns of brain activity in young carriers of the APOE-epsilon4 allele. *Proc Natl Acad Sci U S A*, *106*(17), 7209-7214. https://doi.org/10.1073/pnas.0811879106

Fischer, D., Snider, S. B., Barra, M. E., Sanders, W. R., Rapalino, O., Schaefer, P., Foulkes, A. S., Bodien, Y. G., & Edlow, B. L. (2021). Disorders of Consciousness Associated With COVID-19: A Prospective, Multimodal Study of Recovery and Brain Connectivity. *Neurology*. https://doi.org/10.1212/wnl.0000000000013067

Fischer, D., Threlkeld, Z. D., Bodien, Y. G., Kirsch, J. E., Huang, S. Y., Schaefer, P. W., Rapalino, O., Hochberg, L. R., Rosen, B. R., & Edlow, B. L. (2020). Intact Brain Network Function in an Unresponsive Patient with COVID-19. *Annals of Neurology*, *88*(4), 851-854. https://doi.org/10.1002/ana.25838

Fox, M. D., Snyder, A. Z., Vincent, J. L., Corbetta, M., Van Essen, D. C., & Raichle, M. E. (2005). The human brain is intrinsically organized into dynamic, anticorrelated functional networks. *Proc Natl Acad Sci U S A*, *102*(27), 9673-9678. https://doi.org/10.1073/pnas.0504136102

Fox, M. D., Snyder, A. Z., Zacks, J. M., & Raichle, M. E. (2006). Coherent spontaneous activity accounts for trial-to-trial variability in human evoked brain responses. *Nat Neurosci*, *9*(1), 23-25. https://doi.org/10.1038/nn1616

Friston, K. J., Williams, S., Howard, R., Frackowiak, R. S., & Turner, R. (1996). Movement-related effects in fMRI time-series. *Magn Reson Med*, *35*(3), 346-355.

Friston, K. J. (1994). Functional and effective connectivity in neuroimaging: a synthesis. *Hum Brain Mapp*, *2*(1-2), 56-78.

Friston, K. J., Frith, C. D., Liddle, P. F., & Frackowiak, R. S. (1993). Functional connectivity: the principal-component analysis of large (PET) data sets. *Journal of Cerebral Blood Flow & Metabolism*, *13*(1), 5-14.

Fu, Z., Tu, Y., Calhoun, V. D., Zhang, Y., Zhao, Q., Chen, J., Meng, Q., Lu, Z., & Hu, L. (2021). Dynamic functional network connectivity associated with post-traumatic stress symptoms in COVID-19 survivors. *Neurobiology of Stress*, *15*, 100377. https://doi.org/https://doi.org/10.1016/j.ynstr.2021.100377

Garrigues, E., Janvier, P., Kherabi, Y., Le Bot, A., Hamon, A., Gouze, H., Doucet, L., Berkani, S., Oliosi, E., Mallart, E., Corre, F., Zarrouk, V., Moyer, J. D., Galy, A., Honsel, V., Fantin, B., & Nguyen, Y. (2020). Post-discharge persistent symptoms and health-related quality of life after hospitalization for COVID-19. *J Infect*, *81*(6), e4-e6. https://doi.org/10.1016/j.jinf.2020.08.029

Gay, C. W., Robinson, M. E., Lai, S., O'Shea, A., Craggs, J. G., Price, D. D., & Staud, R. (2016). Abnormal Resting-State Functional Connectivity in Patients with Chronic Fatigue Syndrome: Results of Seed and Data-Driven Analyses. *Brain Connect*, *6*(1), 48-56. https://doi.org/10.1089/brain.2015.0366

Ge, Q., Peng, W., Zhang, J., Weng, X., Zhang, Y., Liu, T., Zang, Y.-F., & Wang, Z. (2017). Short-term apparent brain tissue changes are contributed by cerebral blood flow alterations. *PLoS One*, *12*(8), e0182182. https://doi.org/10.1371/journal.pone.0182182

Glover, G. H. (2011). Overview of functional magnetic resonance imaging. *Neurosurg Clin N Am*, *22*(2), 133-139, vii. https://doi.org/10.1016/j.nec.2010.11.001

Greenhalgh, T., Knight, M., A'Court, C., Buxton, M., & Husain, L. (2020). Management of post-acute covid-19 in primary care. *Bmj*, *370*, m3026. https://doi.org/10.1136/bmj.m3026

Greicius, M. D., Krasnow, B., Reiss, A. L., & Menon, V. (2003). Functional connectivity in the resting brain: a network analysis of the default mode hypothesis. *Proc Natl Acad Sci U S A*, *100*(1), 253-258. https://doi.org/10.1073/pnas.0135058100

Gulko, E., Oleksk, M. L., Gomes, W., Ali, S., Mehta, H., Overby, P., Al-Mufti, F., & Rozenshtein, A. (2020). MRI Brain Findings in 126 Patients with COVID-19: Initial Observations from a Descriptive Literature Review. *American Journal of Neuroradiology*. https://doi.org/10.3174/ajnr.A6805

Hafiz, R., Gandhi, T. K., Mishra, S., Prasad, A., Mahajan, V., Di, X., Natelson, B. H., & Biswal, B. B. (2022). Higher Limbic and Basal Ganglia volumes in surviving COVID-negative patients and the relations to fatigue. *MedRxiv*, 2021.2011.2023.21266761. https://doi.org/10.1101/2021.11.23.21266761

Hafiz, R., Gandhi, T. K., Mishra, S., Prasad, A., Mahajan, V., Natelson, B. H., Di, X., & Biswal, B. B. (2022). Assessing functional connectivity differences and work-related fatigue in surviving COVID-negative patients. *BioRxiv*, 2022.2002.2001.478677. https://doi.org/10.1101/2022.02.01.478677

Helms, J., Kremer, S., Merdji, H., Clere-Jehl, R., Schenck, M., Kummerlen, C., Collange, O., Boulay, C., Fafi-Kremer, S., Ohana, M., Anheim, M., & Meziani, F. (2020). Neurologic Features in Severe SARS-CoV-2 Infection. *New England Journal of Medicine*, *382*(23), 2268-2270. https://doi.org/10.1056/NEJMc2008597

Horwitz, B. (2003). The elusive concept of brain connectivity. *Neuroimage*, *19*(2), 466-470. https://doi.org/https://doi.org/10.1016/S1053-8119(03)00112-5

Inagaki, T. K., Muscatell, K. A., Irwin, M. R., Cole, S. W., & Eisenberger, N. I. (2012). Inflammation selectively enhances amygdala activity to socially threatening images. *Neuroimage*, *59*(4), 3222-3226. https://doi.org/10.1016/j.neuroimage.2011.10.090

Ismail, I. I., & Gad, K. A. (2021). Absent Blood Oxygen Level–Dependent Functional Magnetic Resonance Imaging Activation of the Orbitofrontal Cortex in a Patient With Persistent Cacosmia and Cacogeusia After COVID-19 Infection. *The Journal of the American Medical Association Neurology*. https://doi.org/10.1001/jamaneurol.2021.0009

Kalcher, K., Huf, W., Boubela, R. N., Filzmoser, P., Pezawas, L., Biswal, B., Kasper, S., Moser, E., & Windischberger, C. (2012). Fully exploratory network independent component analysis of the 1000 functional connectomes database. *Front Hum Neurosci*, *6*, 301. https://doi.org/10.3389/fnhum.2012.00301

Kandemirli, S. G., Dogan, L., Sarikaya, Z. T., Kara, S., Akinci, C., Kaya, D., Kaya, Y., Yildirim, D., Tuzuner, F., Yildirim, M. S., Ozluk, E., Gucyetmez, B., Karaarslan, E., Koyluoglu, I., Demirel Kaya, H. S., Mammadov, O., Kisa Ozdemir, I., Afsar, N., Citci Yalcinkaya, B., . . . Kocer, N. (2020). Brain MRI Findings in Patients in the Intensive Care Unit with COVID-19 Infection. *Radiology*, *297*(1), E232-e235. https://doi.org/10.1148/radiol.2020201697

Kang, L., Zhang, A., Sun, N., Liu, P., Yang, C., Li, G., Liu, Z., Wang, Y., & Zhang, K. (2018). Functional connectivity between the thalamus and the primary somatosensory cortex in major depressive disorder: a resting-state fMRI study. *BMC Psychiatry*, *18*(1), 339. https://doi.org/10.1186/s12888-018-1913-6

Keller, E., Brandi, G., Winklhofer, S., Imbach, L. L., Kirschenbaum, D., Frontzek, K., Steiger, P., Dietler, S., Haeberlin, M., Willms, J., Porta, F., Waeckerlin, A., Huber, M., Abela, I. A., Lutterotti, A., Stippich, C., Globas, C., Varga, Z., & Jelcic, I. (2020). Large and Small Cerebral Vessel Involvement in Severe COVID-19: Detailed Clinical Workup of a Case Series. *Stroke*, *51*(12), 3719-3722. https://doi.org/10.1161/strokeaha.120.031224

Kim, B. H., Shin, Y. B., Kyeong, S., Lee, S. K., & Kim, J. J. (2018). Disrupted salience processing involved in motivational deficits for real-life activities in patients with schizophrenia. *Schizophr Res*, *197*, 407-413. https://doi.org/10.1016/j.schres.2018.01.019

Krams, M., Quinton, R., Ashburner, J., Friston, K. J., Frackowiak, R. S. J., Bouloux, P.-M. G., & Passingham, R. E. (1999). Kallmann's syndrome. Mirror movements associated with bilateral corticospinal tract hypertrophy, *Neurology* 1999 Vol. 52(4), 816-816. https://doi.org/10.1212/wnl.52.4.816

Kremer, S., Lersy, F., Anheim, M., Merdji, H., Schenck, M., Oesterlé, H., Bolognini, F., Messie, J., Khalil, A., Gaudemer, A., Carré, S., Alleg, M., Lecocq, C., Schmitt, E., Anxionnat, R., Zhu, F., Jager, L., Nesser, P., Mba, Y. T., . . . Cotton, F. (2020). Neurologic and neuroimaging findings in patients with COVID-19: A retrospective multicenter study. *Neurology*, *95*(13), e1868-e1882. https://doi.org/10.1212/wnl.0000000000010112

Laurendon, T., Radulesco, T., Mugnier, J., Gérault, M., Chagnaud, C., El Ahmadi, A.-A., & Varoquaux, A. (2020). Bilateral transient olfactory bulb edema during COVID-19–related anosmia. *Neurology*, *95*(5), 224-225. https://doi.org/10.1212/wnl.0000000000009850

Lavagnino, L., Amianto, F., D'Agata, F., Huang, Z., Mortara, P., Abbate-Daga, G., Marzola, E., Spalatro, A., Fassino, S., & Northoff, G. (2014). Reduced resting-state functional connectivity of the somatosensory cortex predicts psychopathological symptoms in women with bulimia nervosa. *Frontiers in Behavioral Neuroscience*, *8*, 270-270. https://doi.org/10.3389/fnbeh.2014.00270

Li, C.-W., Syue, L.-S., Tsai, Y.-S., Li, M.-C., Lo, C.-L., Tsai, C.-S., Chen, P.-L., Ko, W.-C., & Lee, N.-Y. (2020). Anosmia and olfactory tract neuropathy in a case of COVID-19. *Journal of Microbiology, Immunology and Infection*. https://doi.org/https://doi.org/10.1016/j.jmii.2020.05.017

Li, H., Liu, L., Zhang, D., Xu, J., Dai, H., Tang, N., Su, X., & Cao, B. (2020). SARS-CoV-2 and viral sepsis: observations and hypotheses. *The Lancet*, *395*(10235), 1517-1520. https://doi.org/10.1016/S0140-6736(20)30920-X

Li, Y. C., Bai, W. Z., Hirano, N., Hayashida, T., Taniguchi, T., Sugita, Y., Tohyama, K., & Hashikawa, T. (2013). Neurotropic virus tracing suggests a membranous-coating-mediated mechanism for transsynaptic communication. *J Comp Neurol*, *521*(1), 203-212. https://doi.org/10.1002/cne.23171

Liu, P., Yang, W., Zhuang, K., Wei, D., Yu, R., Huang, X., & Qiu, J. (2021). The functional connectome predicts feeling of stress on regular days and during the COVID-19 pandemic. *Neurobiol Stress*, *14*, 100285. https://doi.org/10.1016/j.ynstr.2020.100285

Logue, J. K., Franko, N. M., McCulloch, D. J., McDonald, D., Magedson, A., Wolf, C. R., & Chu, H. Y. (2021). Sequelae in Adults at 6 Months After COVID-19 Infection. *The Journal of the American Medical Association Netw Open*, *4*(2), e210830. https://doi.org/10.1001/jamanetworkopen.2021.0830

Lowe, M. J., Mock, B. J., & Sorenson, J. A. (1998). Functional connectivity in single and multislice echoplanar imaging using resting-state fluctuations. *Neuroimage*, *7*(2), 119-132. https://doi.org/10.1006/nimg.1997.0315

Lu, Y., Li, X., Geng, D., Mei, N., Wu, P.-Y., Huang, C.-C., Jia, T., Zhao, Y., Wang, D., Xiao, A., & Yin, B. (2020). Cerebral Micro-Structural Changes in COVID-19 Patients; An MRI-based 3-month Follow-up Study. *EClinicalMedicine*, *25*. https://doi.org/10.1016/j.eclinm.2020.100484

Lüders, E., Steinmetz, H., & Jäncke, L. (2002). Brain size and grey matter volume in the healthy human brain. *Neuroreport*, 13(17):2371-4. doi: 10.1097/01.wnr.0000049603.85580.da. PMID: 12488829.

Malayala, S. V., Jaidev, P., Vanaparthy, R., & Jolly, T. S. (2021). Acute COVID-19 Cerebellitis: A Rare Neurological Manifestation of COVID-19 Infection. *Cureus*, *13*(10), e18505-e18505. https://doi.org/10.7759/cureus.18505

Matsuda, H. (2016). MRI morphometry in Alzheimer's disease. *Ageing Res Rev*, *30*, 17-24. https://doi.org/10.1016/j.arr.2016.01.003

Matsuda, K., Park, C. H., Sunden, Y., Kimura, T., Ochiai, K., Kida, H., & Umemura, T. (2004). The vagus nerve is one route of transneural invasion for intranasally inoculated influenza a virus in mice. *Vet Pathol*, *41*(2), 101-107. https://doi.org/10.1354/vp.41-2-101

Mattioli, P., Pardini, M., Famà, F., Girtler, N., Brugnolo, A., Orso, B., Meli, R., Filippi, L., Grisanti, S., Massa, F., Bauckneht, M., Miceli, A., Terzaghi, M., Morbelli, S., Nobili, F., & Arnaldi, D. (2021). Cuneus/precuneus as a central hub for brain functional connectivity of mild cognitive impairment in idiopathic REM sleep behavior patients. *Eur J Nucl Med Mol Imaging*, *48*(9), 2834-2845. https://doi.org/10.1007/s00259-021-05205-6

May, A., Ashburner, J., Büchel, C., McGonigle, D. J., Friston, K. J., Frackowiak, R. S. J., & Goadsby, P. J. (1999). Correlation between structural and functional changes in brain in an idiopathic headache syndrome. *Nature Medicine*, *5*(7), 836-838. https://doi.org/10.1038/10561

McCray, P. B., Jr., Pewe, L., Wohlford-Lenane, C., Hickey, M., Manzel, L., Shi, L., Netland, J., Jia, H. P., Halabi, C., Sigmund, C. D., Meyerholz, D. K., Kirby, P., Look, D. C., & Perlman, S. (2007). Lethal infection of K18-hACE2 mice infected with severe acute respiratory syndrome coronavirus. *J Virol*, *81*(2), 813-821. https://doi.org/10.1128/jvi.02012-06

McKeown, M. J., Makeig, S., Brown, G. G., Jung, T. P., Kindermann, S. S., Bell, A. J., & Sejnowski, T. J. (1998). Analysis of fMRI data by blind separation into independent spatial components. *Hum Brain Mapp*, *6*(3), 160-188. https://doi.org/10.1002/(SICI)1097-0193(1998)6:3<160::AID-HBM5>3.0.CO;2-1

Meier, T. B., Wildenberg, J. C., Liu, J., Chen, J., Calhoun, V. D., Biswal, B. B., Meyerand, M. E., Birn, R. M., & Prabhakaran, V. (2012). Parallel ICA identifies sub-components of resting state networks that covary with behavioral indices. *Front Hum Neurosci*, *6*, 281. https://doi.org/10.3389/fnhum.2012.00281

Miller, A. H., Jones, J. F., Drake, D. F., Tian, H., Unger, E. R., & Pagnoni, G. (2014). Decreased basal ganglia activation in subjects with chronic fatigue syndrome: association with symptoms of fatigue. *PLoS One*, *9*(5), e98156. https://doi.org/10.1371/journal.pone.0098156

Natelson, B. H. (2019). Myalgic Encephalomyelitis/Chronic Fatigue Syndrome and Fibromyalgia: Definitions, Similarities, and Differences. Clinical Therapeutics, 41(4), 612-618. https://doi.org/https://doi.org/10.1016/j.clinthera.2018.12.016

National Center for Immunization and Respiratory Diseases (NCIRD), D. o. V. D. (2020, December 22, 2020). *Symptoms of Coronavirus*. Centers for Disease Control and Prevention (CDC). Retrieved 02/02/2021 from https://www.cdc.gov/coronavirus/2019-ncov/symptoms-testing/symptoms.html

Nemoto, K. (2017). [Voxel-Based Morphometry for Schizophrenia: A Review]. *Brain Nerve*, *69*(5), 513-518. https://doi.org/10.11477/mf.1416200777

Neuromorphometrics, I. *Building a Model of the Living Human Brain*. Retrieved 02/24/2022 from http://www.neuromorphometrics.com/?page_id=38

Nicholson, P., Alshafai, L., & Krings, T. (2020). Neuroimaging Findings in Patients with COVID-19. *American Journal of Neuroradiology*, *41*(8), 1380-1383. https://doi.org/10.3174/ajnr.A6630

Niesen, M., Trotta, N., Noel, A., Coolen, T., Fayad, G., Leurkin-Sterk, G., Delpierre, I., Henrard, S., Sadeghi, N., Goffard, J.-C., Goldman, S., & De Tiège, X. (2021). Structural and metabolic brain abnormalities in COVID-19 patients with sudden loss of smell. *European journal of nuclear medicine and molecular imaging*, *48*(6), 1890-1901. https://doi.org/10.1007/s00259-020-05154-6

Ogawa, S., Lee, T. M., Kay, A. R., & Tank, D. W. (1990). Brain magnetic resonance imaging with contrast dependent on blood oxygenation. *Proc Natl Acad Sci U S A*, *87*(24), 9868-9872. https://doi.org/10.1073/pnas.87.24.9868

Paterson, R. W., Brown, R. L., Benjamin, L., Nortley, R., Wiethoff, S., Bharucha, T., Jayaseelan, D. L., Kumar, G., Raftopoulos, R. E., Zambreanu, L., Vivekanandam, V., Khoo, A., Geraldes, R., Chinthapalli, K., Boyd, E., Tuzlali, H., Price, G., Christofi, G., Morrow, J., . . . Zandi, M. S. (2020). The emerging spectrum of COVID-19 neurology: clinical, radiological and laboratory findings. *Brain*, *143*(10), 3104-3120. https://doi.org/10.1093/brain/awaa240

Pellicano, C., Gallo, A., Li, X., Ikonomidou, V. N., Evangelou, I. E., Ohayon, J. M., Stern, S. K., Ehrmantraut, M., Cantor, F., McFarland, H. F., & Bagnato, F. (2010). Relationship of Cortical Atrophy to Fatigue in Patients With Multiple Sclerosis. *Archives of Neurology*, *67*(4), 447-453. https://doi.org/10.1001/archneurol.2010.48

Peluso, M. J., Kelly, J. D., Lu, S., Goldberg, S. A., Davidson, M. C., Mathur, S., Durstenfeld, M. S., Spinelli, M. A., Hoh, R., Tai, V., Fehrman, E. A., Torres, L., Hernandez, Y., Williams, M. C., Arreguin, M. I., Bautista, J. A., Ngo, L. H., Deswal, M., Munter, S. E., . . . Martin, J. N. (2021). Rapid implementation of a cohort for the study of post-acute sequelae of SARS-CoV-2 infection/COVID-19. *MedRxiv*, 2021.2003.2011.21252311. https://doi.org/10.1101/2021.03.11.21252311

Perica, M. I., Ravindranath, O., Calabro, F. J., Foran, W., & Luna, B. (2021). Hippocampal-Prefrontal Connectivity Prior to the COVID-19 Pandemic Predicts Stress Reactivity. *Biol Psychiatry Glob Open Sci*, *1*(4), 283-290. https://doi.org/10.1016/j.bpsgos.2021.06.010

Politi, L. S., Salsano, E., & Grimaldi, M. (2020). Magnetic Resonance Imaging Alteration of the Brain in a Patient With Coronavirus Disease 2019 (COVID-19) and Anosmia. *The Journal of the American Medical Association Neurol*, *77*(8), 1028-1029. https://doi.org/10.1001/jamaneurol.2020.2125

Power, J. D., Barnes, K. A., Snyder, A. Z., Schlaggar, B. L., & Petersen, S. E. (2012). Spurious but systematic correlations in functional connectivity MRI networks arise from subject motion. *Neuroimage*, *59*(3), 2142-2154. https://doi.org/10.1016/j.neuroimage.2011.10.018

Puntmann, V. O., Carerj, M. L., Wieters, I., Fahim, M., Arendt, C., Hoffmann, J., Shchendrygina, A., Escher, F., Vasa-Nicotera, M., Zeiher, A. M., Vehreschild, M., & Nagel, E. (2020). Outcomes of Cardiovascular Magnetic Resonance Imaging in Patients Recently Recovered From Coronavirus Disease 2019 (COVID-19). *The Journal of the American Medical Association Cardiol*, *5*(11), 1265-1273. https://doi.org/10.1001/jamacardio.2020.3557

Qin, Y., Wu, J., Chen, T., Li, J., Zhang, G., Wu, D., Zhou, Y., Zheng, N., Cai, A., Ning, Q., Manyande, A., Xu, F., Wang, J., & Zhu, W. (2021). Long-term microstructure and cerebral blood flow changes in patients recovered from COVID-19 without neurological manifestations. *J Clin Invest*, *131*(8). https://doi.org/10.1172/jci147329

Raichle, M. E., & Mintun, M. A. (2006). Brain work and brain imaging. *Annu Rev Neurosci*, *29*, 449-476. https://doi.org/10.1146/annurev.neuro.29.051605.112819

RStudio. (2021). *RStudio Team (2021). RStudio: Integrated Development for R. http://www.rstudio.com/.* In RStudio.

Scarpazza, C., Nichols, T. E., Seramondi, D., Maumet, C., Sartori, G., & Mechelli, A. (2016). When the Single Matters more than the Group (II): Addressing the Problem of High False Positive Rates in Single Case Voxel Based Morphometry Using Non-parametric Statistics. *Front Neurosci*, *10*, 6-6. https://doi.org/10.3389/fnins.2016.00006

Sergeeva, M., Rech, J., Schett, G., & Hess, A. (2015). Response to peripheral immune stimulation within the brain: magnetic resonance imaging perspective of treatment success. *Arthritis Research & Therapy*, *17*(1), 268. https://doi.org/10.1186/s13075-015-0783-2

Shah, P. J., Ebmeier, K. P., Glabus, M. F., & Goodwin, G. M. (1998). Cortical grey matter reductions associated with treatment-resistant chronic unipolar depression: Controlled magnetic resonance imaging study. *British Journal of Psychiatry*, *172*(6), 527-532. https://doi.org/10.1192/bjp.172.6.527

Shirer, W. R., Ryali, S., Rykhlevskaia, E., Menon, V., & Greicius, M. D. (2012). Decoding subject-driven cognitive states with whole-brain connectivity patterns. *Cereb Cortex*, *22*(1), 158-165. https://doi.org/10.1093/cercor/bhr099

Shulman, R. G., Rothman, D. L., Behar, K. L., & Hyder, F. (2004). Energetic basis of brain activity: implications for neuroimaging. *Trends Neurosci*, *27*(8), 489-495. https://doi.org/10.1016/j.tins.2004.06.005

Smith, S. M., Fox, P. T., Miller, K. L., Glahn, D. C., Fox, P. M., Mackay, C. E., Filippini, N., Watkins, K. E., Toro, R., Laird, A. R., & Beckmann, C. F. (2009). Correspondence of the brain's functional architecture during activation and rest. *Proceedings of the National Academy of Sciences*, *106*(31), 13040-13045. https://doi.org/10.1073/pnas.0905267106

Soudry, Y., Lemogne, C., Malinvaud, D., Consoli, S. M., & Bonfils, P. (2011). Olfactory system and emotion: Common substrates. *European Annals of Otorhinolaryngology, Head and Neck Diseases*, *128*(1), 18-23. https://doi.org/https://doi.org/10.1016/j.anorl.2010.09.007

Tabacof, L., Tosto-Mancuso, J., Wood, J., Cortes, M., Kontorovich, A., McCarthy, D., Rizk, D., Mohammadi, N., Breyman, E., Nasr, L., Kellner, C., & Putrino, D. (2020). Post-acute COVID-19 syndrome negatively impacts health and wellbeing despite less severe acute infection. *MedRxiv*, 2020.2011.2004.20226126. https://doi.org/10.1101/2020.11.04.20226126

Taylor, P. A., & Saad, Z. S. (2013). FATCAT: (an efficient) Functional and Tractographic Connectivity Analysis Toolbox. *Brain Connect*, *3*(5), 523-535. https://doi.org/10.1089/brain.2013.0154

Tu, Y., Zhang, Y., Li, Y., Zhao, Q., Bi, Y., Lu, X., Kong, Y., Wang, L., Lu, Z., & Hu, L. (2021). Post-traumatic stress symptoms in COVID-19 survivors: a self-report and brain imaging follow-up study. *Molecular Psychiatry*. https://doi.org/10.1038/s41380-021-01223-w

van Schouwenburg, M. R., den Ouden, H. E., & Cools, R. (2015). Selective attentional enhancement and inhibition of fronto-posterior connectivity by the basal ganglia during attention switching. *Cereb Cortex*, *25*(6), 1527-1534. https://doi.org/10.1093/cercor/bht345

Vargha-Khadem, F., Watkins, K. E., Price, C. J., Ashburner, J., Alcock, K. J., Connelly, A., Frackowiak, R. S. J., Friston, K. J., Pembrey, M. E., Mishkin, M., Gadian, D. G., & Passingham, R. E. (1998). Neural basis of an inherited speech and language disorder. *Proceedings of the National Academy of Sciences*, *95*(21), 12695-12700. https://doi.org/10.1073/pnas.95.21.12695

Wang, L., Wang, K., Liu, J.-H., & Wang, Y.-P. (2018). Altered Default Mode and Sensorimotor Network Connectivity With Striatal Subregions in Primary Insomnia: A Resting-State Multi-Band fMRI Study [Original Research]. *Front Neurosci*, *12*(917). https://doi.org/10.3389/fnins.2018.00917

Woermann, F. G., Free, S. L., Koepp, M. J., Ashburner, J., & Duncan, J. S. (1999). Voxel-by-Voxel Comparison of Automatically Segmented Cerebral Gray Matter—A Rater-Independent Comparison of Structural MRI in Patients with Epilepsy. *Neuroimage*, *10*(4), 373-384. https://doi.org/https://doi.org/10.1006/nimg.1999.0481

Wortinger, L. A., Glenne Øie, M., Endestad, T., & Bruun Wyller, V. (2017). Altered right anterior insular connectivity and loss of associated functions in adolescent chronic fatigue syndrome. *PLoS One*, *12*(9), e0184325. https://doi.org/10.1371/journal.pone.0184325

Wright, I. C., Ellison, Z. R., Sharma, T., Friston, K. J., Murray, R. M., & McGuire, P. K. (1999). Mapping of grey matter changes in schizophrenia1This work was presented, in part, at the VIth International Congress on Schizophrenia Research, Colorado Springs, Colorado, USA, April 1997.1. *Schizophrenia Research*, *35*(1), 1-14. https://doi.org/https://doi.org/10.1016/S0920-9964(98)00094-2

Wright, I. C., McGuire, P. K., Poline, J. B., Travere, J. M., Murray, R. M., Frith, C. D., Frackowiak, R. S. J., & Friston, K. J. (1995). A Voxel-Based Method for the Statistical Analysis of Gray and White Matter Density Applied to Schizophrenia. *Neuroimage*, *2*(4), 244-252. https://doi.org/https://doi.org/10.1006/nimg.1995.1032

Wylie, G. R., Dobryakova, E., DeLuca, J., Chiaravalloti, N., Essad, K., & Genova, H. (2017). Cognitive fatigue in individuals with traumatic brain injury is associated with caudate activation. *Sci Rep*, *7*(1), 8973. https://doi.org/10.1038/s41598-017-08846-6

Wylie, G. R., Genova, H., Dobryakova, E., DeLuca, J., Chiaravalloti, N., Falvo, M., & Cook, D. (2019). Fatigue in Gulf War Illness is associated with tonically high activation in the executive control network. *Neuroimage Clin*, *21*, 101641. https://doi.org/10.1016/j.nicl.2018.101641

Xiao, M., Chen, X., Yi, H., Luo, Y., Yan, Q., Feng, T., He, Q., Lei, X., Qiu, J., & Chen, H. (2021). Stronger functional network connectivity and social support buffer against negative affect during the COVID-19 outbreak and after the pandemic peak. *Neurobiology of Stress*, *15*, 100418-100418. https://doi.org/10.1016/j.ynstr.2021.100418

Yamasue, H. (2017). [Voxel-Based Morphometry in Autism Spectrum Disorder]. *Brain Nerve*, *69*(5), 529-538. https://doi.org/10.11477/mf.1416200779

Yan, C.-G., Wang, X.-D., Zuo, X.-N., & Zang, Y.-F. (2016). DPABI: Data Processing & Analysis for (Resting-State) Brain Imaging. *Neuroinformatics*, *14*(3), 339-351. https://doi.org/10.1007/s12021-016-9299-4

Yassa, M. A., & Stark, C. E. (2009). A quantitative evaluation of cross-participant registration techniques for MRI studies of the medial temporal lobe. *Neuroimage*, *44*(2), 319-327. https://doi.org/10.1016/j.neuroimage.2008.09.016

Yasuda, C. L., Betting, L. E., & Cendes, F. (2010). Voxel-based morphometry and epilepsy. *Expert Rev Neurother*, *10*(6), 975-984. https://doi.org/10.1586/ern.10.63

Yeo, B. T., Krienen, F. M., Sepulcre, J., Sabuncu, M. R., Lashkari, D., Hollinshead, M., Roffman, J. L., Smoller, J. W., Zöllei, L., Polimeni, J. R., Fischl, B., Liu, H., & Buckner, R. L. (2011). The organization of the human cerebral cortex estimated by intrinsic functional connectivity. *J Neurophysiol*, *106*(3), 1125-1165. https://doi.org/10.1152/jn.00338.2011

Zang, Y. F., He, Y., Zhu, C. Z., Cao, Q. J., Sui, M. Q., Liang, M., Tian, L. X., Jiang, T. Z., & Wang, Y. F. (2007). Altered baseline brain activity in children with ADHD revealed by resting-state functional MRI. *Brain Dev*, *29*(2), 83-91. https://doi.org/10.1016/j.braindev.2006.07.002

Zhang, S., Cui, J., Zhang, Z., Wang, Y., Liu, R., Chen, X., Feng, Y., Zhou, J., Zhou, Y., & Wang, G. (2022). Functional connectivity of amygdala subregions predicts vulnerability to depression following the COVID-19 pandemic. *J Affect Disord*, *297*, 421-429. https://doi.org/10.1016/j.jad.2021.09.107

Zhao, Y. M., Shang, Y. M., Song, W. B., Li, Q. Q., Xie, H., Xu, Q. F., Jia, J. L., Li, L. M., Mao, H. L., Zhou, X. M., Luo, H., Gao, Y. F., & Xu, A. G. (2020). Follow-up study of the pulmonary function and related physiological characteristics of COVID-19 survivors three months after recovery. *EClinicalMedicine*, *25*, 100463. https://doi.org/10.1016/j.eclinm.2020.100463

Zubair, A. S., McAlpine, L. S., Gardin, T., Farhadian, S., Kuruvilla, D. E., & Spudich, S. (2020). Neuropathogenesis and Neurologic Manifestations of the Coronaviruses in the Age of Coronavirus Disease 2019: A Review. *The Journal of the American Medical Association Neurology*, *77*(8), 1018-1027. https://doi.org/10.1001/jamaneurol.2020.2065